

Economic Possibilities of Corrosion-Resistant Low-Alloy Steel in Box Girder Highway Bridges

J. M. HAYES and S. P. MAGGARD

Respectively, Professor of Structural Engineering, Purdue University, and Assistant Professor of Structural Engineering, New Mexico State University

An analytical study was made of the economic possibilities of the use of corrosion-resistant low-alloy steel for girders in composite action with a precast high-strength concrete deck for short and medium length highway bridges. A design procedure is presented. Structural quantities and cost data are developed for one- and three-cell steel boxes for 75- and 120-ft simple spans. The structures involve the integrated use of a nickel-copper grade of ASTM A242 and T-1 steels. Cost data are also given for the use of ASTM A441 steel, as well as of stainless-clad steel for the exterior plates of the steel box.

The results indicate that it is possible to design and erect a box structure for short and medium length highway bridges at a lower first cost than the conventional I-beam highway bridge with a poured-in-place concrete deck. It is recommended that a nickel-copper type of high-strength low-alloy steel be used due to its better resistance to atmospheric corrosion because thin plates are proposed in the steel box.

•THE OBJECTIVE of this work was to investigate the economic possibilities of nickel-copper high-strength alloy steels in short and medium length highway bridges. Two reports on this study have been published previously. In the first (1), designs for the superstructures of typical short-span concrete slab and rolled wide-flange steel stringer highway bridges fabricated from nickel-copper high-strength low-alloy steels were analytically compared with those fabricated from ASTM A7 and A373 structural steels. The results of this first study indicated that this type of highway bridge could, for all practical purposes, be constructed of nickel-copper types of high-strength low-alloy steels at the same first cost in dollars as if ASTM A7 or A373 structural steels were used.

The second report (2) was an analytical study of the comparative economic use of various steels for welded I-section stringers with concrete deck for short and medium length highway bridges within the framework of the standard design specifications. The results indicated that structures of this type could be fabricated and erected using a nickel-copper grade of high-strength low alloy steel at about the same first cost in dollars as if ASTM A373 structural steel were used.

Since the publication of these first two reports, changes in the chemical requirements in the specifications for ASTM A36 structural steel have resulted in its being accepted for welding in highway bridges. It is expected that ASTM A7 and A373 structural steels will be replaced by A36 structural steel. The cost of fabricating and erecting the types of structures covered in these first two reports using ASTM A36 structural steel will average about 95 percent of the same first cost in dollars

if a nickel-copper grade of high-strength low-alloy steel were used. However, it may be possible that the higher atmospheric corrosion resistance of the nickel-copper grades of high-strength low-alloy steels will result in overall economy due to savings in maintenance costs.

This report covers the third phase of the investigation, which was an analytical study of the use of high-strength steels, with particular attention to nickel alloy steels, in forms for short and medium length highway bridges independent of current standard practice and design specifications.

PROPOSED TYPE

Presupposing satisfactory dynamic properties, the most efficient steel highway bridge superstructure is one which incorporates a combination of the various grades of constructional steels with integral action in all directions. Design procedures and fabrication, erection, and maintenance problems must be considered in the overall economic evaluation. The intangible matter of esthetics should also receive attention.

One possible type of construction is a welded steel box girder with a deck unit acting compositely with it. This type results from an attempt to reduce the excess shear carrying capacity of the standard I-beam highway bridge. The deck unit could be either a steel orthotropic plate or a reinforced concrete slab. The types investigated in this study are shown in Figures 1 and 2. It is proposed that a high-strength concrete deck be precast in units of suitable length and held in place with high-strength

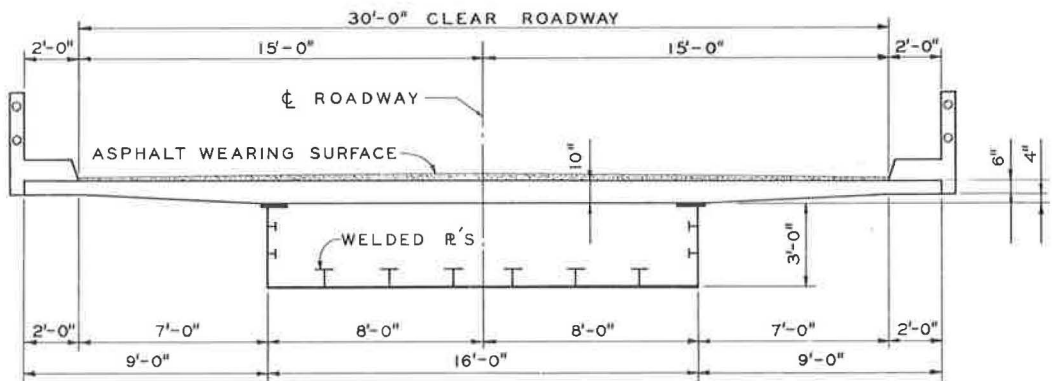


Figure 1. Details of one-cell box.

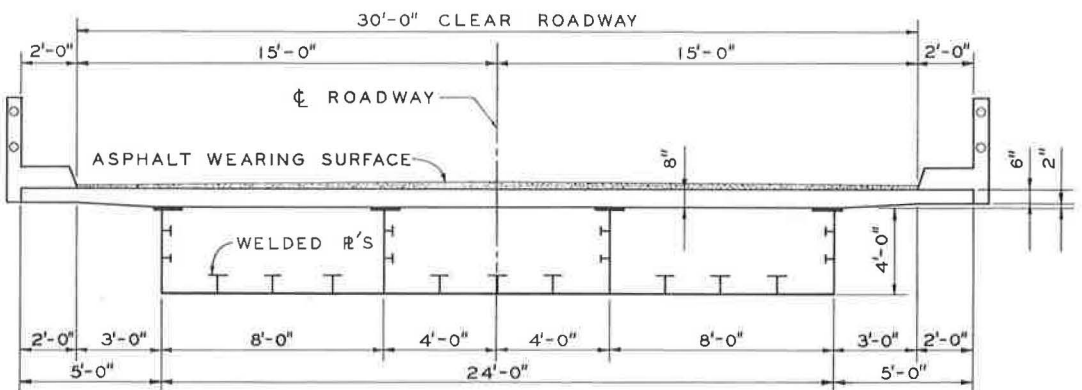


Figure 2. Details of three-cell box.

grout and high-strength bolts to give integral action with either a one- or a three-cell steel box girder. These slab units are joined together with high-strength grout. Post-stressed strand might be feasible to hold the units together. This procedure has been used for highway structures in Europe (3, 4). A combination of high-strength bolts and epoxy resins has been used on one structure in Europe with a span of 7.38 meters, about 24 ft (5). The use of epoxy bonding compounds to secure composite action is being studied at Rensselaer Polytechnic Institute (6).

Steel Box Details

The various grades of constructional steels are combined to give the best possible balanced use of the material in the design of the steel box girder. The plates around the box have one-sided longitudinal stiffeners, which are continuous throughout the

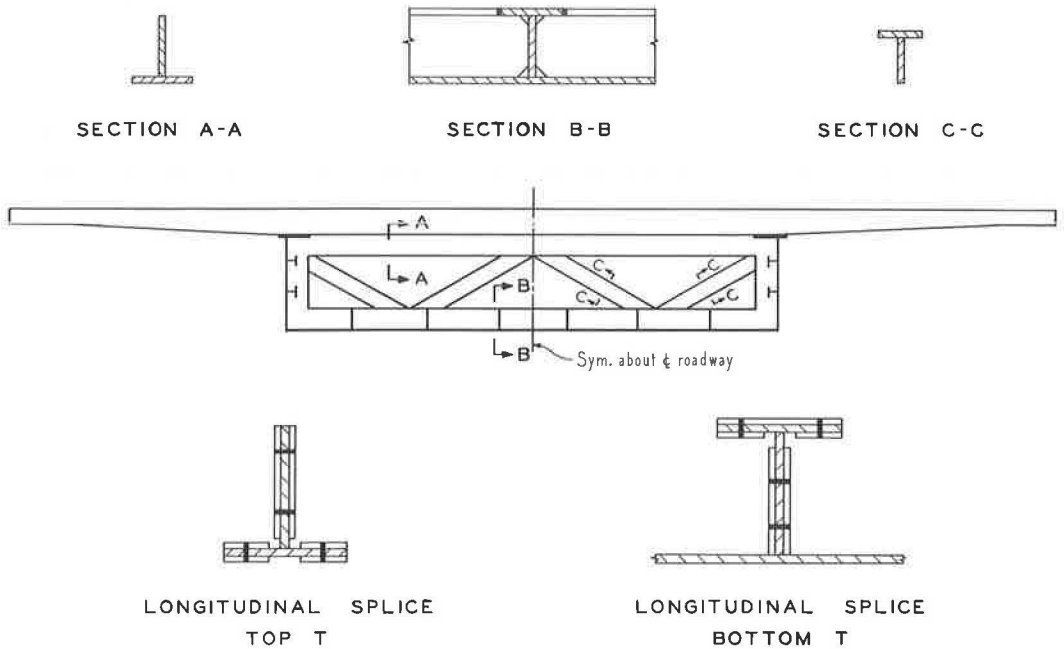


Figure 3. Details of transverse stiffening ring.

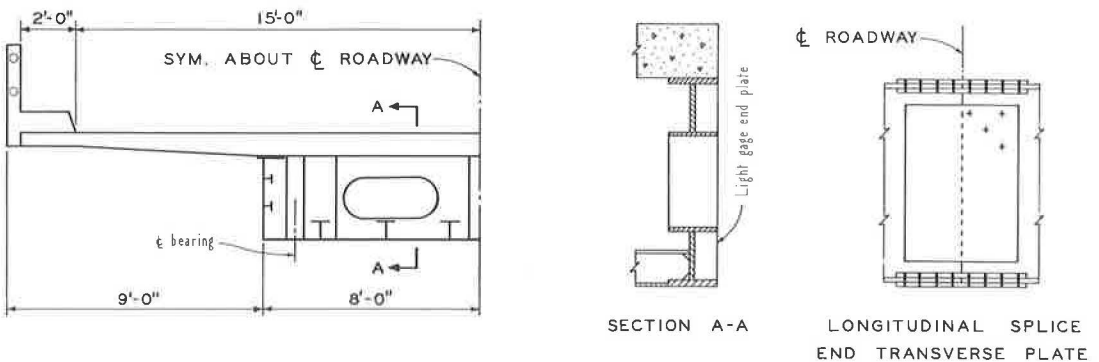


Figure 4. Details of transverse end stiffening ring.

length of the girder and participate in direct structural action with the plates. A rolled structural T may be used for these longitudinal stiffeners instead of a welded T as shown in Figures 1 and 2.

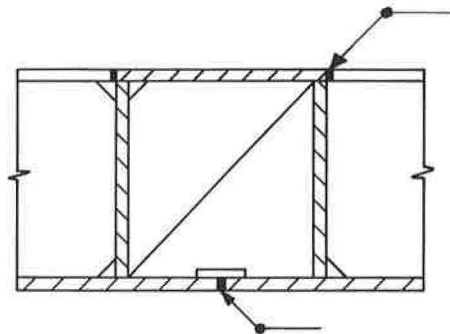
Intermediate transverse stiffening ring diaphragms are spaced at about 12-ft intervals, (Fig. 3). Typical details of a transverse end stiffening ring diaphragm are shown in Figure 4. These details are also typical for a ring at an intermediate support in a continuous structure. At an abutment end, the box is completely sealed with a light gage seal plate. Access to the interior of the box girder is given by covered entrance holes in the bottom plate, near the abutments where the bending moment is small. The bearing details at an end or intermediate support vary, depending on the substructure configuration.

The steel box is shop fabricated into the largest units which can be shipped to a specific site. All shop fabrication is by an appropriate welding procedure and the side plates are joined by butt welding to form appropriate units of the box.

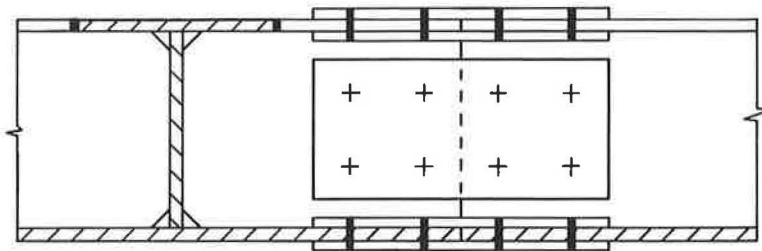
Field Splices

No transverse field splicing is usually required for short and medium length structures. Longitudinal sections, 120 ft long, can be shipped to the site. Details for a transverse splice at a stiffening ring are shown in Figure 5 for use in continuous spans and other places where splices might be required.

Usually longitudinal field splicing is required. The details of a high-strength bolted longitudinal splice are shown in Figure 6. Details of a complete penetration one-sided



WELDED SPLICE



BOLTED SPLICE

Figure 5. Details of transverse splice.

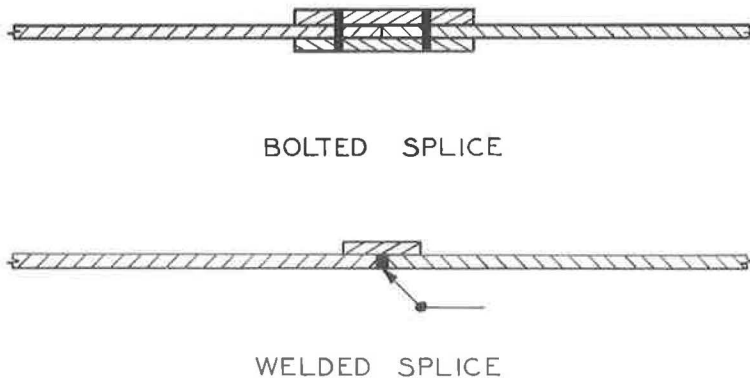


Figure 6. Details of longitudinal splice.

butt weld with backup strip are also shown. The bolted splice is preferred because of ease of erection. The details for the splicing of intermediate and end transverse stiffening rings due to longitudinal splicing are shown in Figures 3 and 4.

THEORETICAL ANALYSIS OF BOX

The units of the steel box, as shop fabricated, have to be braced for shipment to the site. Circumstances vary, and this matter is not given further attention here, because similar situations are now satisfactorily handled.

The complete steel box has to support its own weight and that of the precast slab, either for the full length of a span or between erection bents. It is assumed that the total deadweight of the structure is carried by the steel section and that the live load is carried by the complete cross-section when the precast slab acts compositely with the steel portion of the box girder.

Stress Analysis

The stress analysis of the steel portion of the box girder under the dead load of the structure presents no unusual problems. Both the flexural and the horizontal shear formulas are used, as well as the usual theory for combined stresses.

The stress analysis of the complete box girder under the live load differs somewhat from that of the standard I-beam highway bridge. The primary stresses in this composite section are those due to shear and flexure from symmetrical loading and those due to torsion from unsymmetrical loading, especially live and wind loads.

The precast slab is transformed to an equivalent steel section by using the ratio of the modulus of elasticity of the steel to that of the concrete (E_s/E_c). Using the ratio between the shearing moduli of the two materials gives a coefficient, $G_s/G_c = 0.92 E_s/E_c$.

The membrane analogy (7) is used to determine the shearing stresses due to torsion and to locate the shear center of the box. The so-called shear flow forces (8) are computed by subdividing the cross-section of the box into segments. It is convenient to use segments corresponding to the discontinuities in the static moments caused by the longitudinal stiffeners. This gives an average shear flow force for each segment based on the following assumptions: (a) the plate thickness is small in comparison with other dimensions, (b) there are no re-entrant corners, and (c) the shear is uniform across the plate thickness. Figure 7 shows the distribution of these shear flow forces in the box for both a vertical load through the shear center and a horizontal load through some convenient point.

The loads acting on the box are broken into load through the shear center of the box and torsion about the shear center. The shear flow forces due to torsion are computed by a direct application of the membrane analogy. The shear flow due to torsion is given by:

$$q_t = T/2A_B \quad (1)$$

where

q_t = shear flow force due to torsion (lb/lin in.),

T = applied torsion (in. -lb), and

A_B = area enclosed by box section (sq in.).

The horizontal shearing stress formula may be written:

$$\tau t = VQ/I = q \quad (2)$$

where

τ = unit shearing stress,

t = thickness of plate at point in question,

V = total external shear at the transverse section under consideration,

I = total moment of inertia of the transverse cross-section about its centroidal axis,

Q = statical moment of the cross-sectional area of the transverse cross-section on either side of the point in question about the centroidal axis of the section, and

q = shear flow force per linear measure.

The units must be kept compatible. The box cross-section is assumed to be cut at some convenient point and a quantity q is computed for each segment into which the box is divided. The restoration of the cut section and torsional equilibrium are determined in one operation by taking moments about some convenient point.

Stability Analysis

The steel plates of the box must be stable at all times, both during and after erection. The top plates must have lateral stability until the precast slab units are in

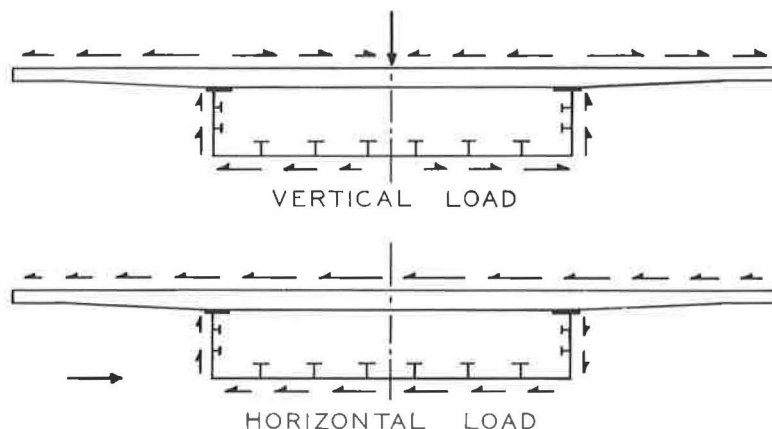


Figure 7. Distribution of shear flow forces.

place. Temporary braces may be used, or a slab unit might be bolted in position to serve as a temporary brace. The size and spacing of the stiffeners must be determined.

The upper limit of the elastic action of a plate may be either the theoretical elastic buckling stress or the yield strength of the material. A plate element, such as one of those comprising the box section, may carry additional load beyond the theoretical elastic buckling strength by transferring the additional load to the edge supports. This is usually referred to as the post-buckling strength of the plate and its magnitude depends on the strength of the edge supports.

In this study the limit of elastic action is used as an upper bound to determine the requirements for the stability of the plates in the steel box. The theoretical elastic buckling stress at which elastic instability takes place is given for a rectangular plate by the Bryan buckling formula (9, 10, 11):

$$\sigma_{cr} \text{ or } \tau_{cr} = \frac{k\pi^2 E}{12(1 - \mu^2)} \left(\frac{t}{b}\right)^2 \quad (3)$$

where

σ_{cr} = critical normal stress due to bending and/or axial load;

τ_{cr} = critical shearing stress;

a = long dimension of rectangular plate element;

b = short dimension of rectangular plate element;

α = aspect ratio, a/b;

E = modulus of elasticity;

μ = Poisson's ratio;

t = thickness of plate element; and

k = constant depending on type of loading, magnitude of aspect ratio, and edge support conditions of plate element.

The plates of the box may be considered as simply supported panels with lengths equal to the spacing of the intermediate transverse stiffening rings and widths equal to the spacing of the longitudinal stiffeners (12). Figure 8 shows the setup for a typical vertical side plate with flexural stress distribution. The setup for shear stress distribution is similar. The horizontal bottom plate will be in tension in a simple span and stability is no problem. In the regions of negative moment in a continuous span, the bottom plate will be in compression and may be treated similarly to the vertical plates.

Using $E = 30,000$ ksi and $\mu = 0.3$, the Bryan buckling formula reduces to σ_{cr} or $\tau_{cr} = 27,114.4k(t/b)^2$ ksi. The constant k may be determined from Table 36 of Bleich (11, Chap. 11). For varying normal stress distribution, linear interpolation may be made between the values of Cases 1 and 2 as given in this table. The theoretical elastic buckling stress for each panel of the side plates must be determined for each stress condition during and after erection. In a simple span the shearing and flexural stresses will not both be a maximum at the same transverse section of the structure and they may be considered separately. It is recommended that in no case should the theoretical elastic buckling stress for any panel be less than 1.5 times the actual comparable flexural or shearing stress in the panel.

High values of flexural and shearing stresses may occur simultaneously at a transverse section in continuous spans. The following interaction relationship may be used to determine safe ratios between the actual stresses and the theoretical elastic buckling stresses for the Panels 11 and 13:

$$\frac{\sigma^D}{\sigma_{cr}^D} + \left(\frac{\sigma^F}{\sigma_{cr}^F} \right)^2 + \left(\frac{\tau}{\tau_{cr}} \right)^2 \leq 0.67 \quad (4)$$

where σ^D , σ^F and τ are, respectively, the actual average direct stress, the maximum flexural stress, and the shearing stress in a panel; and σ_{cr}^D , σ_{cr}^F , and τ_{cr} are the corresponding theoretical elastic buckling stresses for each individual state of stress in the same panel.

Longitudinal Stiffener Rigidity

Based on the stipulation that a longitudinal stiffener remains straight until the theoretical elastic buckling stress is reached, with the panels and edge supports as previously assumed, studies (14, 15) indicate that the required minimum rigidity for a single-sided longitudinal stiffener in the case of pure flexure may be taken as follows:

1. stiffener at mid-depth of plate:

$$I = 0.1167t^3b \quad (5a)$$

2. stiffener at quarter-depth from compression flange:

$$I = t^3b (1.1 + 8.45\delta) (\alpha - 0.3) \quad (5b)$$

with a maximum value of $t^3b (1.4667 + 18.3333\delta)$; and

3. stiffener at one-fifth of the depth from compression flange

$$I = t^3b \left[0.354 + 0.467\alpha + (0.807 + 7.114\delta) \alpha^2 \right] \quad (5c)$$

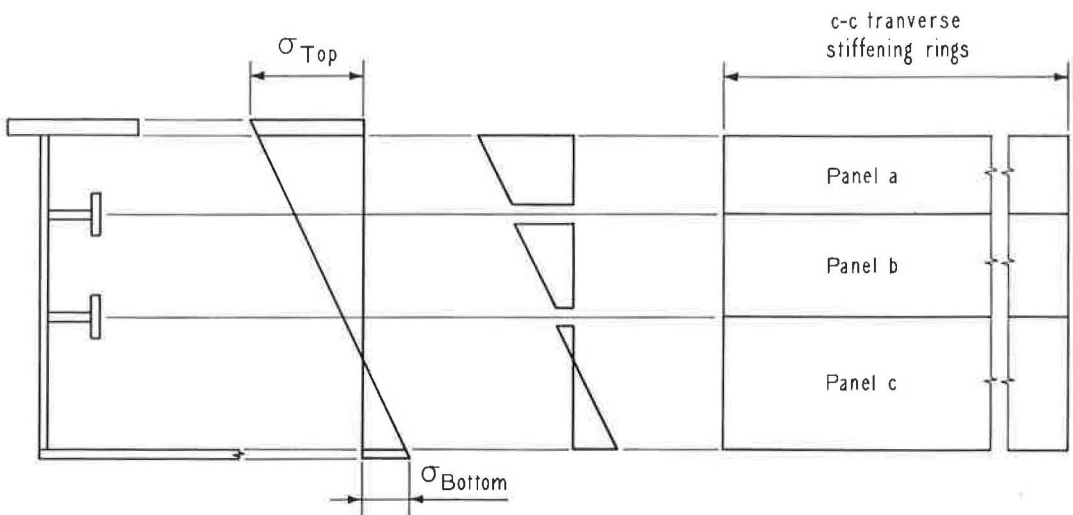
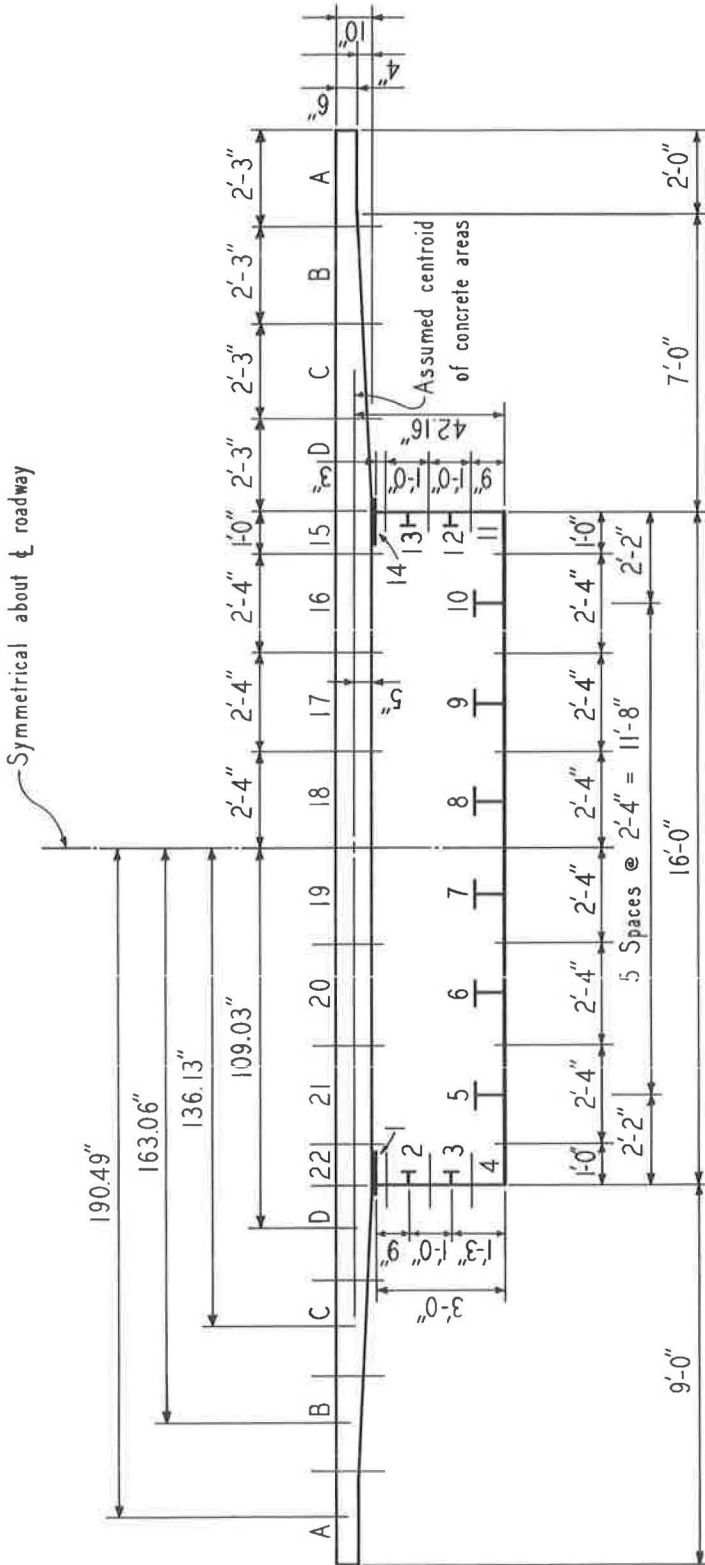


Figure 8. Assumptions for buckling of side plate.



BOX SECTION

- Top Flange ϕ 12 x 1
- Vertical Side ϕ 's 36 x $\frac{1}{4}$
- Bottom ϕ 192 x $\frac{5}{16}$

LONGITUDINAL STIFFENERS

- Vertical Side Plates
- 2 ϕ 's 4 x $\frac{1}{4}$ or Structural T's
- Bottom Side Plates
- 2 ϕ 's 8 x $\frac{5}{16}$ or Structural T's

Figure 9. Analysis details of one-cell box, 75-ft span.

The nomenclature is as previously used with the addition of δ as the ratio of the area of the stiffener to the cross-sectional area of the plate bt , and I as the moment of inertia of the stiffener taken about the surface in contact with the plate.

For the stress distribution as shown in Figure 8, the stiffener rigidity, I , may be computed using the plate width, b , for a hypothetical plate with width equal to twice the greatest distance from the neutral axis to the edge of the plate (12). Shear will not be a consideration in the determination of longitudinal stiffener rigidity for the aspect ratios involved. The minimum size longitudinal stiffener will undoubtedly be controlled by practical considerations and not by stability requirements, since the stiffeners participate in direct structural action with the side plates of the box.

Transverse Stiffening Rings

Transverse stiffening rings are required to help hold the steel box to its original configuration and control the aspect ratio of the side plates. Ring size would be set primarily by practical consideration of the fabrication and erection problems. They would probably be of the same size as the longitudinal stiffeners. Again, either a rolled structural T or a welded T could be used for these rings. It is recommended at present (1963) that width to thickness ratios follow current practice (16).

SUGGESTED DESIGN PROCEDURE FOR ONE-CELL BOX

A suggested design procedure is illustrated by the analysis of a 75-ft simple span structure consisting of a one-cell box for the H20-S16 live loading. The concrete slab must be designed and preliminary thicknesses for the side plates and spacings and sizes for the longitudinal stiffeners estimated. The flexural stresses may be determined from the flexure formula and the shearing stresses, including those due to torsion, computed by an application of the membrane analogy.

The details of the one-cell box for a 75-ft simple span are shown in Figure 9. The box is divided into segments, taken symmetrical with respect to the stiffeners. Segments A, B, C, and D in the cantilever portion of the slab resist shear, but torsion is resisted only by the box section, Segments 1 through 22. A modular ratio, E_s/E_c , of 6 is used for 5,000-psi concrete to obtain the equivalent steel area for the slab segments.

Vertical Load

The computation of the section moduli required to obtain the flexural stresses due to vertical loads and an analysis for the determination of shear flow forces for a shear of 100 kips due to a vertical load through the shear center of the box are given in Table 1. The assumption that each segmental area (Col. 2) is concentrated at the centerline of the side plate is considered to give sufficient accuracy to the computations. Dividing the sum of the vertical distances from each element to the center of the bottom plate, y' , and the first moments of the segmental areas about the center of the bottom plate, Ay' , by the total area locates the centroidal axis from the center of the bottom plate: $\bar{y} = 26,400.26/734.06 = 35.9647$ in. for the composite section; and $\bar{y} = 1,358.04/140.08 = 9.69$ in. for the steel section.

The values of Ay'^2 are for use in the determination of the moments of inertia about the centroidal x-axis from the following:

$$I_x = \sum Ay'^2 - \bar{y}^2 \sum A \quad (6)$$

For the composite section:

$$I_x = 1,099,724.78 - 734.06 (35.9647)^2 = 150,247.79 \text{ in.}^4$$

TABLE 1
VERTICAL LOAD—SHEAR STRESS ANALYSIS, ONE-CELL BOX, 75-FOOT SPAN

1	2	3	4	5	6	7	8	9	10	11	12	13	14	15
Segment	A Area (in ²)	y' Arm From Bot. R. (in.)	AY' (in ³)	Ay' ² (in ⁴)	y' Arm From Comp. C.G. (in.)	AY (in ³)	$\Delta q = \frac{V}{A} \Delta y$ (lb / in.)	q _y (lb / in.)	L Length (in.)	a Arm (in.)	L · a (in ²)	q _y · L · a (lb · in.)	q _y + q _i (lb / in.)	(q _y + q _i) · L (lb)
1	12.75	35.66	467.42	17,135.43	0.5953	8.865	5.900	5.900	9.50	96.00	912.00	5,380.80	1230.518	11,734.21
2	5.00	27.16	135.80	3,696.33	8.8047	-44.024	-23.301	-23.401	12.00	96.00	1152.00	26,957.95	1201.207	14,414.48
3	5.00	15.16	75.80	1,149.13	20.8047	-104.024	-69.235	-69.235	15.16	96.00	1455.36	134,818.73	113.1.982	17,162.85
4	6.04	0.0	0.0	0.0	35.9647	-217.227	-144.579	-237.215	26.00	0.0	0.0	0.0	987.403	25,672.48
5	13.75	0.0	0.0	0.0	35.9647	-494.515	-329.133	-566.348	28.00	0.0	0.0	0.0	658.270	18,431.56
6	13.75	0.0	0.0	0.0	35.9647	-494.515	-329.133	-895.481	28.00	0.0	0.0	0.0	329.137	9,215.84
7	13.75	0.0	0.0	0.0	35.9647	-494.515	-329.133	-1,224.614	28.00	0.0	0.0	0.0	0.0	0.0
8	13.75	0.0	0.0	0.0	35.9647	-494.515	-329.133	-1,553.747	28.00	0.0	0.0	0.0	0.0	0.0
9	13.75	0.0	0.0	0.0	35.9647	-494.515	-329.133	-1,882.860	28.00	0.0	0.0	0.0	0.0	0.0
10	13.75	0.0	0.0	0.0	35.9647	-494.515	-329.133	-2,212.013	26.00	0.0	0.0	0.0	0.0	0.0
11	6.04	0.0	0.0	0.0	35.9647	-217.227	-144.579	-2,356.532	15.16	96.00	1,455.36	3,429,689.73	-1131.974	17,160.73
12	5.00	15.16	75.80	1,149.13	20.8047	-104.024	-69.235	-2,425.827	12.00	96.00	1,152.00	2,794,852.70	-1201.209	14,414.51
13	5.00	27.16	135.80	3,696.33	8.8047	-44.024	-29.301	-2,455.128	9.50	96.00	912.00	2,239,076.74	-1230.510	11,683.85
14	12.75	35.66	467.42	17,135.43	0.6953	8.865	5.900	-2,449.228	5.50	96.00	528.00	1,293,192.38	-1224.610	6,735.36
A	27.03	42.16	1,139.58	48,044.89	6.1953	167.459	111.455	111.455					111.455	
B	30.67	42.16	1,293.05	54,514.81	6.1953	190.010	126.464	237.919					237.919	
C	36.67	42.16	1,546.01	65,179.66	6.1953	227.182	151.204	389.123					389.123	
D	42.61	42.16	1,793.44	75,737.81	6.1953	264.364	175.638	564.821					564.821	
15	20.00	42.16	843.20	35,549.31	6.1953	123.906	82.468	180.1939	26.00	42.16	1,036.16	1,957,213.45	-577.321	15,010.35
16	46.67	42.16	1,967.61	82,954.32	6.1953	289.135	192.439	1,609.500	28.00	42.16	1,180.48	1,999,382.56	-384.882	10,776.70
17	46.67	42.16	1,967.61	82,954.32	6.1953	289.135	192.439	1,417.061	28.00	42.16	1,180.48	1,672,812.17	-192.443	5,388.40
18	46.67	42.16	1,967.61	82,954.32	6.1953	289.135	192.439	1,224.622	28.00	42.16	1,180.48	1,445,641.78	0.0	0.0
19	46.67	42.16	1,967.61	82,954.32	6.1953	289.135	192.439	1,032.183	28.00	42.16	1,180.48	1,218,471.39	192.435	5,388.41
20	46.67	42.16	1,967.61	82,954.32	6.1953	289.135	192.439	859.744	28.00	42.16	1,180.48	991,501.00	384.874	10,776.47
21	46.67	42.16	1,967.61	82,954.32	6.1953	289.135	192.439	647.305	36.00	42.16	1,036.16	709,549.85	577.313	15,010.14
22	20.00	42.16	843.20	35,549.31	6.1953	123.906	82.468	0.0	5.50	96.00	528.00	0.0	1,224.618	6,735.40
D	42.61	42.16	1,793.44	75,737.81	6.1953	264.364	175.638	0.0					564.821	
C	36.67	42.16	1,546.01	65,179.66	6.1953	227.182	151.204	-564.821					-389.123	
D	42.61	42.16	1,793.44	75,737.81	6.1953	264.364	175.638	-389.123					-237.919	
B	30.67	42.16	1,293.05	54,514.81	6.1953	190.010	126.464	-237.919					-111.455	
A	27.03	42.16	1,139.58	48,044.89	6.1953	167.459	111.455	-111.455					-111.455	
Comp. Sec.	734.06		26,400.26	1,099,724.78							16,183.44			19,825,879.63
Steel Sec.	140.08		1358.04	43,945.76							2 A B			

and for the steel section:

$$I_x = 43,945.78 - 140.08(9.69)^2 = 30,792.81 \text{ in.}^4$$

The shear flow forces for a 100-kip shear due to a vertical load through the shear center may now be computed. The box is cut between Segments 22 and 1, and the resulting shear flow forces are computed around the box. The place the box is cut is a matter of convenience. Cutting where $q = 0$ simplifies the computations. The torque of these shear flow forces around a point is determined and used to restore equilibrium and continuity to the box section. The shear flow forces in Segments A, B, C, and D on the left are opposite hand to those on the right and may be neglected in computing any torque. The static moment, Ay , of the segmental area about the centroidal axis of the composite box is computed by using the distance, y , from the centroidal axis to the center of each segment. The average increment in shear flow force acting in each segment of the cut box, $\Delta q = (V/I) Ay$, is given ($V/I = 100,000/150,247.79 = 0.665567194 \text{ lb/in.}^4$).

The intensity of the shear flow force at the center of each segment in the cut section, q_y , is found by summation, beginning with Segment 1, and it is assumed constant between the centers of the segments. The subscript y is used on q to indicate that the shear flow forces are from vertical loads. The shear flow forces create a torque. Since there is no torque with the load acting vertically through the shear center, the forces must be corrected, except for those in Segments A, B, C, and D, and brought into equilibrium. This may be done by determining the torque of the total shear flow forces around the box section about some convenient point and making the necessary correction to reduce the torque to zero. The torque will be computed about the intersection of the centerline of the bottom plate and the vertical centroidal axis of the box; clockwise torque is taken as positive. Columns 10 through 13 of Table 1 contain the computations necessary to determine the correction coefficient to be added algebraically to the values of q_y in Column 9. The distances between the centers of adjacent segments are noted by L . The total shear flow force between the centers of adjacent segments is $q_y L$ and, letting a denote the perpendicular arm to each $q_y L$ from the assumed torque center, the total torque is $\Sigma q_y La$. The correction coefficient, q_1 , is equal to $-\Sigma q_y La / \Sigma La = 19,825,879.63/16,189.44 = 1,224.618 \text{ lb/in.}$, where $\Sigma La = 2A_B$, with A_B being the total area inclosed by the box section.

The corrected values of the shear flow forces from a 100-kip shear due to a vertical load through the shear center, $q_y + q_1$, may be used to determine the shear flow force due to any vertical loading symmetrical with respect to the shear center of the box. The unit shearing stress is obtained by dividing the shear flow force by the thickness in inches of the side plate.

A check for horizontal and vertical equilibrium is obtained by noting that the values of the total shear flow forces, $(q_y + q_1)L$, for segments of opposite hand should have the same magnitude but be of opposite sign. Another check on the computations is to note that twice the area inclosed by the box section, $2A_B$, is $(2)(192)(42.16) = 16,189.44$, which is the same as the summation of Column 12, $\Sigma La = 16,189.44$.

Horizontal Load and Location of Shear Center

In the analysis for a 100-kip horizontal load, it is convenient to assume that the load acts along the horizontal centerline of the bottom side plate of the box. It could be assumed to act along any horizontal line. The computations in Columns 1 through 13 of Table 2 correspond to those in Columns 1 through 15 of Table 1. The location of the vertical centroidal axis is known for the horizontal load. The intensity of the shear flow force at the center of each segment is designated by q_x to indicate that the shear flow force is from a horizontal load. The shear flow forces in Segments A, B, C, and D must be considered, since the shear flow forces on the left and the right cantilever sides of the box act in the same direction. They must not be corrected in

1 Segment	2 A Area (in. ²)	3 X Arm From † Box (in.)	4 A·X (in. ³)	5 A·X ² (in. ⁴)	6 $\Delta q_x = \frac{H}{I} A \cdot X$ (lb/in.)	7 q_x (lb/in.)	8 a Arm (in.)	9 L Length (in.)
1	12.75	96.00	1 224.00	117,504.00	15.90	15.90	96.00	9.50
2	5.00	96.00	480.00	46,080.00	6.24	22.14	96.00	12.00
3	5.00	96.00	480.00	46,080.00	6.24	28.38	96.00	15.16
4	6.04	96.00	579.84	55,664.64	7.53	35.91	0.0	26.00
5	13.75	70.00	962.50	67,375.00	12.50	48.41	0.0	28.00
6	13.75	42.00	577.50	24,255.00	7.50	55.91	0.0	28.00
7	13.75	14.00	192.50	2,695.00	2.50	58.41	0.0	28.00
8	13.75	- 14.00	- 192.50	2,695.00	- 2.50	55.91	0.0	28.00
9	13.75	- 42.00	- 577.50	24,255.00	- 7.50	48.41	0.0	28.00
10	13.75	- 70.00	- 962.50	67,375.00	- 12.50	35.91	0.0	26.00
11	6.04	- 96.00	- 579.84	55,664.64	- 7.53	28.38	96.00	15.16
12	5.00	- 96.00	- 480.00	46,080.00	- 6.24	22.14	96.00	12.00
13	5.00	- 96.00	- 480.00	46,080.00	- 6.24	15.20	96.00	9.50
14	12.75	- 96.00	- 1 224.00	117,504.00	- 15.90	0.0	96.00	5.50
A	27.03	- 190.43	- 5 148.84	980,787.27	- 66.89	- 66.89	42.16	27.43
B	30.67	- 163.06	- 5 001.05	815,524.14	- 64.97	- 131.86	42.16	26.93
C	36.67	- 136.13	- 4 986.59	679,433.54	- 64.83	- 196.69	42.16	27.10
D	42.61	- 109.03	- 4 647.05	508,971.91	- 60.38	- 257.07	42.16	13.03
15	20.00	- 96.00	- 1 920.00	184,320.00	- 24.94	- 282.01	42.16	26.00
16	46.67	- 70.00	- 3 266.90	228,683.00	- 42.44	- 324.45	42.16	28.00
17	46.67	- 42.00	- 1 960.14	82,325.89	- 25.46	- 349.91	42.16	28.00
18	46.67	- 14.00	- 653.38	9,147.32	- 8.43	- 358.40	42.16	28.00
19	46.67	14.00	653.38	9,147.32	8.43	- 349.91	42.16	28.00
20	46.67	42.00	1 960.14	82,325.89	25.46	- 324.45	42.16	28.00
21	46.67	70.00	3 266.90	228,683.00	42.44	- 282.01	42.16	26.00
22	20.00	96.00	1 920.00	184,320.00	24.94	0.0	96.00	5.50
D	42.61	109.03	4 647.05	508,971.91	60.38	- 257.07	42.16	13.03
C	36.67	136.13	4 986.59	679,433.54	64.83	- 196.69	42.16	27.10
B	30.67	163.06	5 001.05	815,524.14	64.97	- 131.86	42.16	26.93
A	27.03	190.43	5 148.84	980,787.27	66.89	- 66.89	42.16	27.43
	734.06			7,607,693.40				

restoring the cut section, as Segments A, B, C, and D do not resist torque. The correction is given by:

$$q_1 = - \Sigma q_x L a / \Sigma L a \tag{7}$$

In this case, $q_1 = 3,656,878.49 / 16,189.44 = 225.88$ lb/in.

Since only Segments 1 through 22 resist torque, the total shear forces in Segments A, B, C, and D must be considered an external load on the box section in location the shear center (Fig. 7). The general expression for the increment in angle of twist at the section is

$$d\theta/dz_1 = (1/2A_B G) \sum_1^{22} q L / t \tag{8a}$$

The increment in angle of twist at the section due to the external loading under consideration is

$$d\theta/dz_2 = (1/2A_B G) \sum_1^{22} (q_x + q_1) L / t \tag{8b}$$

LYSIS, ONE-CELL BOX, 75-FOOT SPAN

11	12	13	14	15	16	17	18	19	20
$q_x \cdot L \cdot a$	$q_x + q_1$	$(q_x + q_1) L$	$(q_x + q_1) \frac{L}{t}$	$\frac{L}{t}$	a'	$L \cdot a'$	$q_x \cdot L \cdot a'$	$q_x + q_2$	$(q_x + q_2) \frac{L}{t}$
(lb-in.)	(lb/in.)	(lb)	(lb/in.)		(in.)	(in ²)	(lb-in.)	(lb/in)	(lb/in.)
14,500.80	241.78	2,296.91	9,187.64	38.00	96.00	912.00	14,500.80	16.79	638.02
25,505.28	248.02	2,976.24	11,904.96	48.00	96.00	1,152.00	25,505.28	23.03	1,105.44
41,303.12	254.26	3,854.58	15,418.33	60.64	96.00	1,455.36	41,303.12	29.27	1,774.93
0.0	261.79	6,806.54	21,780.93	83.20	36.45	947.70	34,031.91	36.80	3,061.76
0.0	274.29	7,680.12	24,576.38	89.60	36.45	1,020.60	49,407.25	49.30	4,417.28
0.0	281.79	7,890.12	25,248.38	89.60	36.45	1,020.60	57,061.75	56.90	5,089.28
0.0	284.29	7,960.12	25,472.38	89.60	36.45	1,020.60	59,613.25	59.30	5,313.28
0.0	281.79	7,890.12	25,248.38	89.60	36.45	1,020.60	57,061.75	56.80	5,089.28
0.0	274.29	7,680.12	24,576.38	89.60	36.45	1,020.60	49,407.25	49.30	4,417.28
0.0	261.79	6,806.54	21,780.93	83.20	36.45	947.70	34,031.91	36.80	3,061.76
41,303.12	254.26	3,854.58	15,418.33	60.64	96.00	1,455.36	41,303.12	29.27	1,774.93
25,505.28	248.02	2,976.24	11,904.96	48.00	96.00	1,152.00	25,505.28	23.03	1,105.44
14,500.80	241.78	2,296.91	9,187.64	38.00	96.00	912.00	14,500.80	16.79	638.02
0.0	225.88	1,242.34	745.40	3.30	96.00	528.00	0.0	0.87	2.87
77,354.94	-66.89	-1,834.79			5.71	156.63	-10,476.98	-66.89	
149,709.89	-131.86	-3,350.99			5.71	153.77	-20,276.11	-131.86	
224,726.19	-196.69	-5,330.30			5.71	154.74	-30,435.81	-196.69	
141,218.83	-257.07	-3,349.62			5.71	74.40	-19,126.01	-257.07	
309,128.08	-56.13	-1,459.38	-875.63	15.60	5.71	148.46	-41,867.20	-281.12	-4,385.47
383,006.74	-98.57	-2,759.96	-1,655.98	16.80	5.71	159.88	-51,873.07	-323.56	-5,435.81
413,061.76	-124.03	-3,472.84	-2,083.70	16.80	5.71	159.88	-55,943.61	-349.02	-5,863.54
423,084.03	-132.52	-3,710.56	-2,226.34	16.80	5.71	159.88	-57,300.99	-357.51	-6,006.17
413,061.76	-124.03	-3,472.84	-2,083.70	16.80	5.71	159.88	-55,943.61	-349.02	-5,863.54
383,006.74	-98.57	-2,759.96	-1,655.98	16.80	5.71	159.88	-51,873.07	-323.56	-5,435.81
309,128.08	-56.13	-1,459.38	-875.63	15.60	5.71	148.46	-41,867.20	-281.12	-4,385.47
0.0	225.88	1,242.34	745.40	3.30	96.00	528.00	0.0	0.87	2.87
141,218.33	-257.07	-3,349.62			5.71	74.40	-19,126.01	-257.07	
224,726.19	-196.69	-5,330.30			5.71	154.74	-30,435.81	-196.69	
149,709.89	-131.86	-3,350.99			5.71	153.77	-20,276.11	-131.86	
77,354.94	-66.89	-1,834.79			5.71	156.63	-10,476.98	-66.89	
656,878.49			231,739.46			16,189.44	-14,065.10		
						2A _B			

The general expression for torque about the shear center is

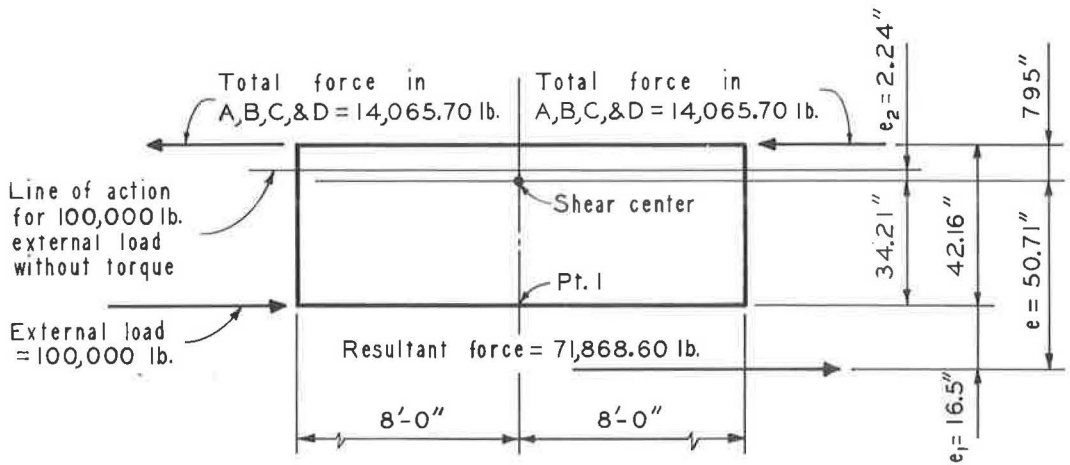
$$T_1 = 2qA_B \tag{9a}$$

The expression for torque about the shear center for the external loading under consideration is

$$T_2 = 71,868.60e \tag{9b}$$

where e is the distance from the resultant force to the shear center (Fig. 10). The computations necessary to locate the shear center are shown in Figure 10. The shear center is the point through which the line of action of the resultant external loading must pass in order to have no torsion. The point of application of the 100-kip horizontal force for zero torque about the shear center is located from $e_2 = (28,131.4) / (7.95) / 100,000 = 2.24$ in. above the shear center (Fig. 10).

The shear flow forces in Column 7 must now be corrected to give torque equilibrium about the shear center with the external load of 100 kips. This load must act 2.24 in. above the shear center for zero torque. This is done by taking the torque of the external load and internal shear flow forces about some convenient point and determining the shear flow corrections to give torque equilibrium about the shear center for the internal shear flow forces. It is convenient to take moments about the line of action of the 100-kip load for zero torque—2.24 in. above the shear center. The correction is found from:



$$\sum H = 0$$

$$100,000 - 2 \times 14,065.70 = 71,868.60 \text{ pounds}$$

$$\sum M \text{ Pt. I}$$

$$e_1 = \frac{2 \times 14,065.70 \times 42.16}{71,868.60} = 16.5''$$

$$\frac{d\theta}{dZ_1} = \frac{1}{2A_B G} \sum_1^{22} q \frac{L}{t}$$

&

$$T_1 = 2q A_B$$

$$\frac{d\theta}{dZ_2} = \frac{1}{2A_B G} \sum_1^{22} (q_x + q_1) \frac{L}{t}$$

&

$$T_2 = 71,868.60 e$$

$$\frac{T_2}{T_1} = \frac{d\theta/dZ_2}{d\theta/dZ_1}$$

$$\frac{71,868.60 e}{16,189.44 q} = \frac{231,739.46}{1,029.48 q}$$

$$e = 50.71''$$

Figure 10. Location of shear center, one-cell box, 75-ft span.

$$q_2 = - \sum q_x La' / \sum La'$$

which is in this case $14,065.10/16,189.44 = 0.87$ lb/in.

Torsion Only

The shear flow force for pure torsion about the shear center is equal to $T/2A_B$. This gives for a pure torsion of 100 ft-kips about the shear center, $q_t = (100,000) (12) / 16,189.44 = 74.12$ lb/in.

Flexural and Shearing Stresses

The dead load per foot of bridge for the one-cell box on the 75-ft span to be used in the stress computations is as follows:

Railing and curb	=	467.4 lb/ft
Asphalt wearing surface	=	450.0 lb/ft
Precast concrete deck	=	3,711.7 lb/ft
Steel box	=	550.7 lb/ft
Total	=	5,179.8 lb/ft

The maximum bending moments and shears for one lane of H20-S16 live loading are given in the AASHO specifications (16, p. 273). The impact factor is 0.25 in accordance with these specifications. The following maximum moments result from full loading of the structure, noting that the maximum live load moment occurs 2.33 ft from mid-span with 14-ft axle spacings for the live load:

$$\begin{aligned} \text{Dead load at mid-span} &= (5.1798) (75)^2/8 = 3,642.1 \text{ ft-kips} \\ \text{Maximum live load plus impact} &= (2) (1075.1) (1.25) = 2,687.8 \text{ ft-kips} \\ \text{Dead load at point of maximum} \\ \text{LL moment} &= \left[(5.1798) (39.83) (35.17) \right] / 2 = \\ &= 3,628.0 \text{ ft-kips} \end{aligned}$$

The following maximum shears occur under the same conditions:

$$\begin{aligned} \text{Dead load at end of span} &= (5.1798) (37.5) = 194.2 \text{ kips} \\ \text{Live load plus impact} &= (2) (63.1) (1.25) = 157.8 \text{ kips} \end{aligned}$$

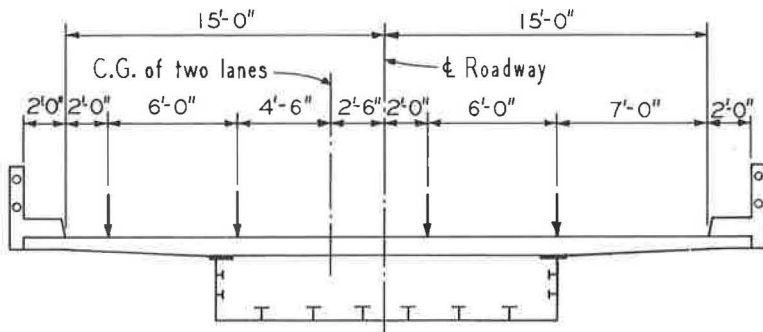


Figure 11. Transverse position of live load for maximum torque.

Torque is obtained by the unsymmetrical placing of the live load lanes on the roadway. Figure 11 shows the transverse position of the live load on the roadway deck for maximum torque, both lanes loaded, with the end heavy axle placed over the support. This gives the value of the maximum live load plus impact torque, with the value of the torque from each load distributed to the end similarly to its effect on end shear as:

$$\left[(64) (2.5) + (64) (2.5) (61) / 75 \right. \\ \left. + (16) (2.5) (47) / 75 \right] (1.25) = 393.75 \text{ ft-kips.}$$

Assuming the dead load carried by the steel box alone and the live load and impact by the total composite section and using the moments of inertia previously computed to obtain the appropriate section moduli yields the unit flexural stresses given in Table 3.

By assuming the dead load shear to be uniformly distributed in the vertical side plates, and determining the maximum live load, impact and torque shearing effect by the use of the coefficients previously determined, the unit shearing stresses between Segments 1 and 2 are as follows:

$$\begin{aligned} \text{DL} &= (194.2) / (2) (36) (1/4) = 10.79 \text{ ksi} \\ \text{LL} + \text{I} &= (1.578) (1.230518) / (1/4) = 7.76 \text{ ksi} \\ \text{Torque} &= (3.9375) (0.07412) / (1/4) = 1.17 \text{ ksi} \\ \hline \text{Total} &= 19.72 \text{ ksi} \end{aligned}$$

SUGGESTED DESIGN PROCEDURE FOR THREE-CELL BOX

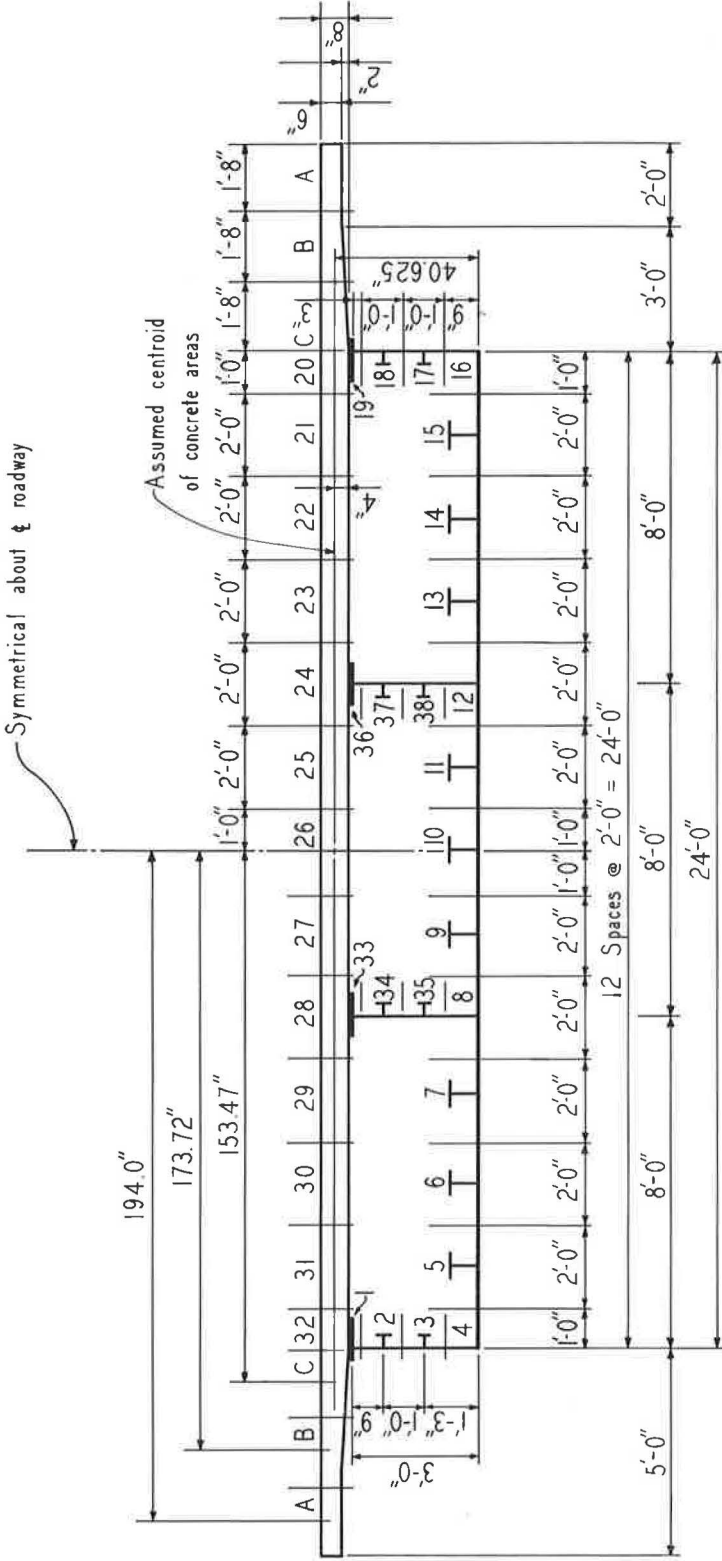
The details of a three-cell box for a 75-ft simple span are shown in Figure 12. The box is divided into 32 segments around the cells with each cantilever portion of the slab divided into Segments A, B, and C, which resist shear but not torsion.

Vertical Load

Tables 4 through 7 contain most of the computations for the effect of a shear of 100 kips due to a vertical load through the shear center of the box. The nomenclature is the same as used for the analysis of the one-cell box. Columns 1 through 5 of Table 4 give the data for the location of the centroids of both the steel box alone and the composite section and the determination of the moments of inertia of each I_x about the centroidal axes. It is necessary to cut the three-cell box into three one-cell boxes

TABLE 3
FLEXURAL STRESSES, ONE-CELL BOX, 75-FOOT SPAN

Load	Top of Steel (ksi)	Bottom of Steel (ksi)	Top of Concrete (ksi)
Dead Load	38.84	13.93	-
Live Load and Impact	<u>0.26</u>	<u>7.76</u>	<u>0.40</u>
Total	39.10	21.69	0.40



- BOX SECTION
 - Top Flange Φ 12 x $\frac{1}{2}$
 - Vertical Side Φ 's 36 x $\frac{3}{16}$
 - Bottom Φ 288 x $\frac{1}{4}$
- LONGITUDINAL STIFFENERS
 - Vertical Side Plates
 - 2 Φ 's 4 x $\frac{1}{4}$ or Structural T's
 - Bottom Side Plates
 - 2 Φ 's 8 x $\frac{5}{16}$ or Structural T's

Figure 12. Analysis details of three-cell box, 75-ft span.

TABLE 5
DEFORMATIONS IN LEFT CELL

Segment	q total (lb/in.)	L (in.)	t (in.)	L/t	q total - L/t
1-2	15.466 + q ₁	9.25	.1875	49.333	762.984 + 49.333 q ₁
2-3	2.482 + q ₁	12.00	.1875	64.000	158.848 + 64.00 q ₁
3-4	-40.345 + q ₁	15.125	.1875	80.667	-3,254.510 + 80.667 q ₁
4-5	-129.493 + q ₁	24.00	.250	96.00	-12,431.328 + 96.00 q ₁
5-6	-337.694 + q ₁	24.00	.250	96.00	-32,418.624 + 96.00 q ₁
6-7	-545.895 + q ₁	24.00	.250	96.00	-52,405.920 + 96.00 q ₁
7-8	-754.096 + q ₁	24.00	.250	96.00	-72,393.216 + 96.00 q ₁
8-35	q ₁ - q ₂	15.125	.1875	80.667	80.667 q ₁ - 80.667 q ₂
35-34	-42.827 + q ₁ - q ₂	12.00	.1875	64.00	-2,740.928 + 64.00 q ₁ - 64.00 q ₂
34-33	-55.811 + q ₁ - q ₂	9.250	.1875	49.333	-2,753.324 + 49.333 q ₁ - 49.333 q ₂
33-28	-40.345 + q ₁ - q ₂	4.250	1.333	3.188	-128.620 + 3.188 q ₁ - 3.188 q ₂
28-29	-864.770 + q ₁	24.00	1.333	18.00	-15,565.860 + 18.00 q ₁
29-30	-709.747 + q ₁	24.00	1.333	18.00	-12,775.446 + 18.00 q ₁
30-31	-554.724 + q ₁	24.00	1.333	18.00	-9,985.032 + 18.00 q ₁
31-32	-399.701 + q ₁	24.00	1.333	18.00	-7,194.618 + 18.00 q ₁
32-1	q ₁	4.25	1.333	3.188	3.188 q ₁
$2A_B \frac{d\theta}{dz} =$					-223,125.588 + 850.376 q ₁ - 197.188 q ₂

TABLE 6
DEFORMATIONS IN MIDDLE CELL

Segment	q total (lb/in.)	L (in.)	t (in.)	L/t	q total - L/t
8-9	- 899.648 + q ₂	24.0	.250	96.00	- 86,366.208 + 96.00 q ₂
9-10	-1,107.849 + q ₂	24.0	.250	96.00	-106,353.504 + 96.00 q ₂
10-11	-1,316.050 + q ₂	24.0	.250	96.00	-126,340.800 + 96.00 q ₂
11-12	-1,524.251 + q ₂	24.0	.250	96.00	-146,328.096 + 96.00 q ₂
12-38	+ q ₂ - q ₃	15.125	.1875	80.667	+ 80.667 q ₂ - 80.667 q ₃
38-37	- 42.827 + q ₂ - q ₃	12.00	.1875	64.00	- 2,740.928 + 64.00 q ₂ - 64.00 q ₃
37-36	- 55.811 + q ₂ - q ₃	9.25	.1875	49.333	- 2,753.324 + 49.333 q ₂ - 49.333 q ₃
36-24	- 40.345 + q ₂ - q ₃	4.25	1.333	3.188	- 128.620 + 3.188 q ₂ - 3.188 q ₃
24-25	-1,444.517 + q ₂	24.00	1.333	18.00	- 26,001.306 + 18.00 q ₂
25-26	-1,289.494 + q ₂	24.00	1.333	18.00	- 23,210.892 + 18.00 q ₂
26-27	-1,134.471 + q ₂	24.00	1.333	18.00	- 20,420.478 + 18.00 q ₂
27-28	- 979.448 + q ₂	24.00	1.333	18.00	- 17,630.074 + 18.00 q ₂
28-33	40.345 + q ₂ - q ₁	4.25	1.333	3.188	128.620 - 3.188 q ₁ + 3.188 q ₂
33-34	55.811 + q ₂ - q ₁	9.25	.1875	49.333	2,753.324 - 49.333 q ₁ + 49.333 q ₂
34-35	42.827 + q ₂ - q ₁	12.00	.1875	64.00	2,740.928 - 64.00 q ₁ + 64.00 q ₂
35-8	q ₂ - q ₁	15.125	.1875	80.667	- 80.667 q ₁ + 80.667 q ₂

$$2 A_B \frac{d\theta}{dz} = - 552,651.36 - 197.188 q_1 + 850.376 q_2 - 197.188 q_3$$

TABLE 7
DEFORMATIONS IN RIGHT CELL

Segment	q total (lb/in)	L (in)	t (in)	L/t	q total - L/t
12-13	-1,669.803 + q ₃	24.0	.25	96.00	-160,301.088 + 96.0 q ₃
13-14	-1,878.004 + q ₃	24.0	.25	96.00	-180,288.384 + 96.0 q ₃
14-15	-2,086.205 + q ₃	24.0	.25	96.00	-200,275.680 + 96.0 q ₃
15-16	-2,294.406 + q ₃	24.0	.25	96.00	-220,262.976 + 96.0 q ₃
16-17	-2,383.590 + q ₃	15.125	.1875	80.667	-192,277.055 + 80.667 q ₃
17-18	-2,426.417 + q ₃	12.0	.1875	64.00	-155,290.688 + 64.00 q ₃
18-19	-2,439.401 + q ₃	9.25	.1875	49.333	-120,342.970 + 49.333 q ₃
19-20	-2,423.935 + q ₃	4.25	1.333	3.188	- 7,727.504 + 3.188 q ₃
20-21	-2,024.264 + q ₃	24.0	1.333	18.00	- 36,436.752 + 18.0 q ₃
21-22	-1,969.241 + q ₃	24.0	1.333	18.00	- 33,646.338 + 18.0 q ₃
22-23	-1,714.218 + q ₃	24.0	1.333	18.00	- 30,855.924 + 18.0 q ₃
23-24	-1,559.195 + q ₃	24.0	1.333	18.00	- 28,065.510 + 18.0 q ₃
24-36	40.345 + q ₃ - q ₂	4.25	1.333	3.188	128.620 - 3.188 q ₂ + 3.188 q ₃
36-37	55.911 + q ₃ - q ₂	9.25	.1875	49.333	2,753.324 - 49.333 q ₂ + 49.333 q ₃
37-38	42.827 + q ₃ - q ₂	12.0	.1875	64.00	2,740.928 - 64.0 q ₂ + 64.0 q ₃
38-12	q ₃ - q ₂	15.125	.1875	80.667	- 80.667 q ₂ + 80.667 q ₃

$$2 A_B \frac{d\theta}{dz} = - 1,360,148.00$$

$$-197.188 q_2 + 850.376 q_3$$

TABLE 9
DEFORMATIONS IN LEFT CELL

Segment	q total (lb/in.)	L/t	q total - L/t
1-2	11.454 + q ₁	49.333	565.060 + 49.333 q ₁
2-3	18.875 + q ₁	64.000	1,208.000 + 64.000 q ₁
3-4	26.296 + q ₁	80.667	2,121.219 + 80.667 q ₁
4-5	34.629 + q ₁	96.000	3,324.384 + 96.000 q ₁
5-6	50.635 + q ₁	96.000	4,860.960 + 96.000 q ₁
6-7	63.440 + q ₁	96.000	6,090.240 + 96.000 q ₁
7-8	73.044 + q ₁	96.000	7,012.224 + 96.000 q ₁
8-35	q ₁ - q ₂	80.667	80.667 q ₁ - 80.667 q ₂
35-34	2.474 + q ₁ - q ₂	64.000	158.336 + 64.000 q ₁ - 64.000 q ₂
34-33	4.948 + q ₁ - q ₂	49.333	244.100 + 49.333 q ₁ - 49.333 q ₂
33-28	8.766 + q ₁ - q ₂	3.188	27.946 + 3.188 q ₁ - 3.188 q ₂
28-29	- 278.579 + q ₁	18.000	- 5,014.422 + 18.000 q ₁
29-30	- 250.642 + q ₁	18.000	- 4,511.556 + 18.000 q ₁
30-31	- 213.392 + q ₁	18.000	- 3,841.056 + 18.000 q ₁
31-32	- 166.830 + q ₁	18.000	- 3,002.940 + 18.000 q ₁
32-1	+ q ₁	3.188	3.188 q ₁

$$2 A_B \frac{d\theta}{dz} = 9,242.495 + 850.376 q_1 - 197.188 q_2$$

TABLE 10
DEFORMATIONS IN MIDDLE CELL

Segment	q total (lb/in.)	L/t	q total - L/t
8-9	77.520 + q ₂	96.00	7,441.920 + 96.00 q ₂
9-10	80.721 + q ₂	96.00	7,749.216 + 96.00 q ₂
10-11	80.721 + q ₂	96.00	7,749.216 + 96.00 q ₂
11-12	77.520 + q ₂	96.00	7,441.920 + 96.00 q ₂
12-33	+ q ₂ - q ₃	80.667	+ 80.667 q ₂ - 80.667 q ₃
33-37	- 2.474 + q ₂ - q ₃	64.00	- 158.336 + 64.000 q ₂ - 64.000 q ₃
37-36	- 4.948 + q ₂ - q ₃	49.333	- 244.100 + 49.333 q ₂ - 49.333 q ₃
36-24	- 8.766 + q ₂ - q ₃	3.188	- 27.946 + 3.188 q ₂ - 3.188 q ₃
24-25	- 305.970 + q ₂	18.00	- 5,507.460 + 18.00 q ₂
25-26	- 315.283 + q ₂	18.00	- 5,675.094 + 18.00 q ₂
26-27	- 315.283 + q ₂	18.00	- 5,675.094 + 18.00 q ₂
27-28	- 305.970 + q ₂	18.00	- 5,507.460 + 18.00 q ₂
28-33	- 8.766 + q ₂ - q ₁	3.188	- 27.946 - 3.188 q ₁ + 3.188 q ₂
33-34	- 4.948 + q ₂ - q ₁	49.333	- 244.100 - 49.333 q ₁ + 49.333 q ₂
34-35	- 2.474 + q ₂ - q ₁	64.00	- 158.336 - 64.00 q ₁ + 64.00 q ₂
35-8	q ₂ - q ₁	80.667	- 80.667 q ₁ + 80.667 q ₂

$$2 A_B \frac{d\theta}{dz} = 7,156.400 - 197.188 q_1 + 850.376 q_2 - 197.188 q_3$$

TABLE 11
DEFORMATIONS IN RIGHT CELL

Segment	q total (lb/in.)	L/t	q total - L/t
12-13	73.044 + q ₃	96.00	7,012.224 + 96.00 q ₃
13-14	63.440 + q ₃	96.00	6,090.240 + 96.00 q ₃
14-15	50.635 + q ₃	96.00	4,860.960 + 96.00 q ₃
15-16	34.629 + q ₃	96.00	3,324.384 + 96.00 q ₃
16-17	26.296 + q ₃	80.667	2,121.219 + 80.667 q ₃
17-18	18.875 + q ₃	64.00	1,208.000 + 64.00 q ₃
18-19	11.454 + q ₃	49.333	565.060 + 49.333 q ₃
19-20	+ q ₃	3.188	+ 3.188 q ₃
20-21	-166.830 + q ₃	18.00	-3,002.940 + 18.00 q ₃
21-22	-213.392 + q ₃	18.00	-3,841.056 + 18.00 q ₃
22-23	-250.642 + q ₃	18.00	-4,511.556 + 18.00 q ₃
23-24	-278.579 + q ₃	18.00	-5,014.422 + 18.00 q ₃
24-36	8.766 + q ₃ - q ₂	3.188	27.946 - 3.188 q ₂ + 3.188 q ₃
36-37	4.948 + q ₃ - q ₂	49.333	244.100 - 49.333 q ₂ + 49.333 q ₃
37-38	2.474 + q ₃ - q ₂	64.000	158.336 - 64.000 q ₂ + 64.000 q ₃
38-12	q ₃ - q ₂	80.667	- 80.667 q ₂ + 80.667 q ₃

$$2 A_B \frac{d\theta}{dz} = 9,242.495 - 197.188 q_2 + 850.376 q_3$$

the box. Again the three-cell box is cut into three one-cell boxes and the shear flow forces are computed as given in Columns 1 through 7 of Table 8. The shear flow forces in Segments A, B, and C must be considered because the shear flow forces on the left and right cantilever sides of the box act in the same direction. They must not be corrected in restoring the cut sections because Segments A, B, and C do not resist torque; also, the total shear flow forces in Segments A, B, and C must be considered as an external load on the box to locate the shear center.

Columns 8, 10, 11, and 12 of Table 8 and Tables 9, 10, and 11 contain the basic data for the restoration of the cut sections to equilibrium about the centerline of the bottom plate on the vertical centerline of the box. The summation of Column 9 in Table 8 is a check on horizontal equilibrium of the section under the 100-kip horizontal load. Again $-\Sigma q_x La / \Sigma La = q_1 + q_2 + q_3$, with $\Sigma La = 2A_B$, twice the area of each cell. This yield $q_1 + q_2 + q_3 = 3,122,041.54/7,800 = 400.2617$.

As before, the other two necessary equations are based on the principle of consistent displacements. Tables 9 and 10 yield $9,242.495 + 850.376q_1 - 197.188q_2 = 7,156.400 - 197.188q_1 + 850.376q_2 - 197.188q_3$. Tables 10 and 11 yield $7,156.400 - 197.188q_1 + 850.376q_2 - 197.188q_3 = 9,242.495 - 197.188q_2 - 850.376q_3$. These two equations reduce to $1,047.564q_1 - 1,047.564q_2 + 197.188q_3 = -2, -86.095$ and $-197.188q_1 + 1,047.564q_2 - 1,047.564q_3 = 2,086.095$. Their solution gives $q_1 = 124.919$ lb/in., $q_2 = 150.424$ lb/in., and $q_3 = 124.919$ lb/in. Thus, $(2A_B G) (d\theta_1/dz) = 9,242.495 + 850.376(124.919) - 197.188(150.424) = 85,808.81$ and $(2A_B G) (d\theta_2/dz) = 7,156.394 - 197.188(124.919) + 850.376(150.424) - 197.188(124.919) = 85,808.29$.

It is now necessary to compute the shear flow forces for pure torque about the shear center. Using an external torque of 1,200,000 in.-lb, with the three-cell box cut to give three single cells, it is seen from the data in Tables 9, 10, and 11 that the deformations due to torque are $(2A_B G) (d\theta_1/dz) = 850.376q_{T1} - 197.188q_{T2}$, $(2A_B G) (d\theta_2/dz) = -197.188q_{T1} + 850.376q_{T2} - 197.188q_{T3}$, and $(2A_B G) (d\theta_3/dz) = -197.188q_{T2} + 850.376q_{T3}$. By letting $d\theta_1/dz = d\theta_2/dz$ and $d\theta_2/dz = d\theta_3/dz$, and noting that $2A_B (q_{T1} + q_{T2} + q_{T3}) = 1,200,000$ where $2A_B = 7,800$ there results $q_{T1} = 48.254$ lb/in., $q_{T2} = 57.338$ lb/in., and $q_{T3} = 48.254$ lb/in. Thus, $(2A_B G) (d\theta_1/dz) = 850.376(48.254) - 197.188(57.338) = 29,727.678$. These shear flow forces are used to determine the shear flow forces due to a pure torque of 100,000 ft-lb about the shear center. The final shear flow forces due to this 100,000 ft-lb torque about the shear center are given in Column 17 of Table 8.

The shear center is located by noting that the torque of the shear flow forces given in Column 7 of Table 8 must be zero about the shear center. The deformations $(2A_B G) (d\theta/dz)$ are not proportional to the torques involved. Thus, the magnitude of the torque, T, which must be reduced to zero is $T = (d\theta_1/dz) (1,200,000) / (d\theta_1/dz)_T = (85,808.29) (1,200,000) / 29,727.678 = 3,463,773.6$ in.-lb.

The total shear flow force in Segments A, B, and C due to the 100-kip horizontal load is 8,286.886 lb (Fig. 13; Table 8, Col. 9). The resultant force is 100,000 - 8,286.886 = 91,713.114 lb, and it must be applied to balance the 8,286.886 lb force in Segments A, B, and C about the line of application of the 100-kip load on the horizontal centerline of the bottom plate. Thus, the resultant is applied at a distance of $e_1 = (8,286.886) (40.625) / (91,713.114) = 3.671$ in. below the centerline of the bottom plate. This gives the distance from this point to the shear center of $e = 3,463,773.6 / 91,713.114 = 37.767$ in., which places the shear center as shown in Figure 13. The point of application of the 100-kip horizontal load for zero torque about the shear center is computed from $e_2 = (8,286.886) (6.529) / 100,000 = 0.541$ in. above the shear center (Fig. 13).

The shear flow forces in Column 7 of Table 8 must be corrected to give torque equilibrium about the shear center in combination with the 100-kip external horizontal load. The external load of 100 kips must act at 0.541 in. above the shear center for zero torque. This is done by taking the torque of the external load and the internal shear flow forces about some convenient point and determining the shear flow correction to give torque equilibrium about the shear center for the internal shear flow forces. It is convenient to take moments about the line of action of the 100-kip load. Again

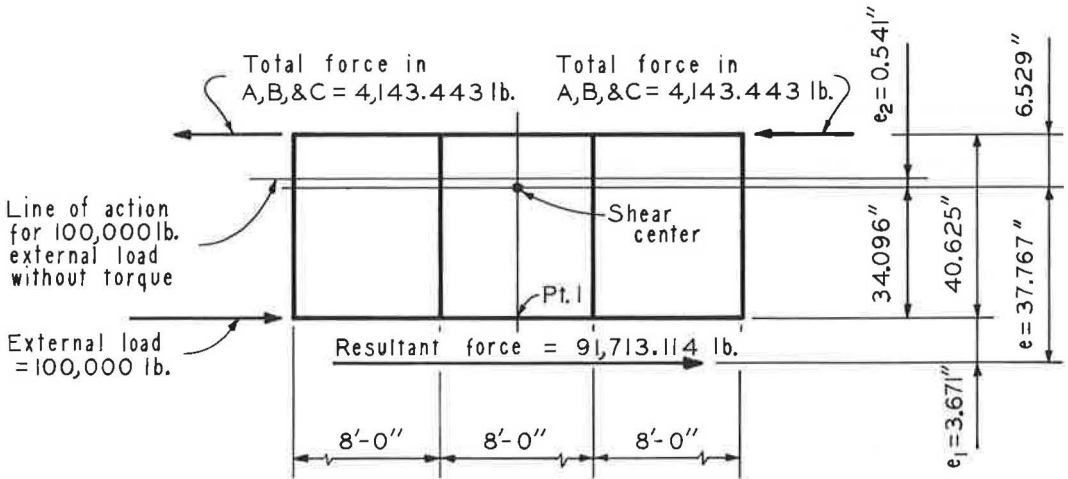


Figure 13. Location of shear center, three-cell box, 75-ft span.

$-\Sigma q_x L a' / \Sigma L a' = q_1' + q_2' + q_3'$, with $\Sigma L a' = 2A_B$ for each cell. Thus, $q_1' + q_2' + q_3' = -341,658.608/7,800 = -43.8024$. Again, based on the principle of consistent displacements, Tables 8, 9, and 10 yield $1,047.564q_1' - 1,047.564q_2' + 197.188q_3' = -2,086.095$ and $-197.188q_1' + 1,047.564q_2' - 1,047.564q_3' = 2,086.095$. Solution of these gives $q_1' = -14.363$ lb/in., $q_2' = -15.076$ lb/in., and $q_3' = -14.363$ lb/in. These corrections are applied to the shear forces in Column 7 of Table 8 to give the corrected shear flow forces for the 100-kip load with zero torque about the shear center as given in Column 16 of Table 8.

Flexural and Shearing Stresses

The dead load per foot of bridge for the three-cell box on the 75-ft span to be used in the stress computations is as follows:

Railing and curb	=	467.4 lb/ft
Asphalt wearing surface	=	450.0 lb/ft
Precast Concrete Deck	=	3,232.5 lb/ft
Steel box	=	743.1 lb/ft
Total	=	<u>4,893.0 lb/ft</u>

The maximum bending moments and shears for one lane of H20-S16 live loading are given in the AASHTO specifications (16, p. 273). The impact factor is 0.25 in accordance with these specifications. The following maximum moments result from full loading of the structure, noting that the maximum live load moment occurs 2.33 ft from mid-span with 14-ft axle spacings for the live load:

Dead load at mid-span	=	$(4.893)(75)^2/8 = 3,440.4$ ft-kips
Maximum live load plus impact	=	$(2)(1075.1)(1.25) = 2,687.8$ ft-kips
Dead load at point of maximum LL moment	=	$\left[(4.893)(39.83)(35.17) \right] / 2 = 3,427.1$ ft-kips

The following maximum shears occur under the same conditions:

$$\begin{aligned}\text{Dead load at end of span} &= (4.893)(37.5) = 183.5 \text{ kips} \\ \text{Live load plus impact} &= (2)(63.1)(1.25) = 157.8 \text{ kips}\end{aligned}$$

The torque resulting from the unsymmetrical placing of the live load lanes on the roadway is the same as for the one-cell box—393.75 ft-kips. With the same assumptions as for the one-cell box, the unit flexural stresses are given in Table 12. Assuming the dead load shear to be uniformly distributed in the vertical plates, and determining the maximum live load and impact and torque shearing effect by the use of the coefficients previously determined, the unit shearing stresses between Segments 36 and 37 are as follows:

$$\begin{aligned}\text{DL} &= (183.5) / (4)(36)(3/16) = 6.80 \text{ ksi} \\ \text{LL} + \text{I} &= (1.578)(0.724341) / (3/16) = 6.10 \text{ ksi} \\ \text{Torque} &= (3.9375)(0.009804) / (3/16) = \underline{0.21 \text{ ksi}} \\ \text{Total} &= 13.11 \text{ ksi}\end{aligned}$$

STABILITY ANALYSIS FOR ONE- AND THREE-CELL BOXES

The steel boxes acting alone in the carrying of the total dead load give the critical condition for the stability of the top flange and side plates. The theoretical elastic buckling stresses may be obtained with the Bryan buckling formula, Eq. 3, with $27,114.4k(t/b)^2$, as previously given.

Top Flange Plates

The top flange plates are assumed to have three simply supported edges and one free edge. The value of $k = 0.43$ is found by Bleich (11, p. 330). This gives $\sigma_{CR} = (27,114.4)(1/9)^2(0.43) = 143.9$ ksi, as compared to the actual extreme fiber stress of 38.8 ksi due to dead load for the one-cell box on the 75-ft span. It also gives $\sigma_{CR} = (27,114.4)(0.5/9)^2(0.43) = 72.0$ ksi, as compared to the actual total extreme fiber stress of 31.53 ksi due to dead load for the three-cell box on the 75-ft span. It also gives $\sigma_{CR} = (27,114.4)(0.5/9)^2(0.43) = 72.0$ ksi, as compared to the actual total extreme fiber stress of 31.53 ksi due to dead load for the three-cell box on the 75-ft span.

Vertical Side Plates

The dead load flexural stresses for the panel subdivisions of the vertical side plates for both the one- and three-cell boxes on the 75-ft span are shown in Figure 14. The

TABLE 12
FLEXURAL STRESSES, THREE-CELL BOX, 75-FOOT SPAN

Load	Top of Steel (ksi)	Bottom of Steel (ksi)	Top of Concrete (ksi)
Dead Load	31.53	10.55	
Live Load and Impact	<u>0.81</u>	<u>6.13</u>	<u>0.39</u>
Total	32.34	16.68	0.39

theoretical elastic buckling stresses and comparisons with the actual maximum flexural stresses are given in Tables 13 and 14.

The theoretical elastic buckling stresses for the case of shear are given in Tables 15 and 16, as well as the comparisons with the actual total shearing stresses in each panel. The coefficient $k = 5.3$ is used for computing these buckling stresses due to shear.

Deflection Limitations

The total moments of inertia which a two-lane superstructure needs to meet the live load and impact deflection limitations of present standard specifications for highway bridges (16) are shown in Figure 15. Also shown are the moments of inertia furnished by the final composite structure for 75- and 120-ft spans with both one- and three-cell boxes. The basic background of this figure was presented previously (2, Fig. 4). It is evident that the steel box structures meet current practice with respect to live load and impact deflection limitations.

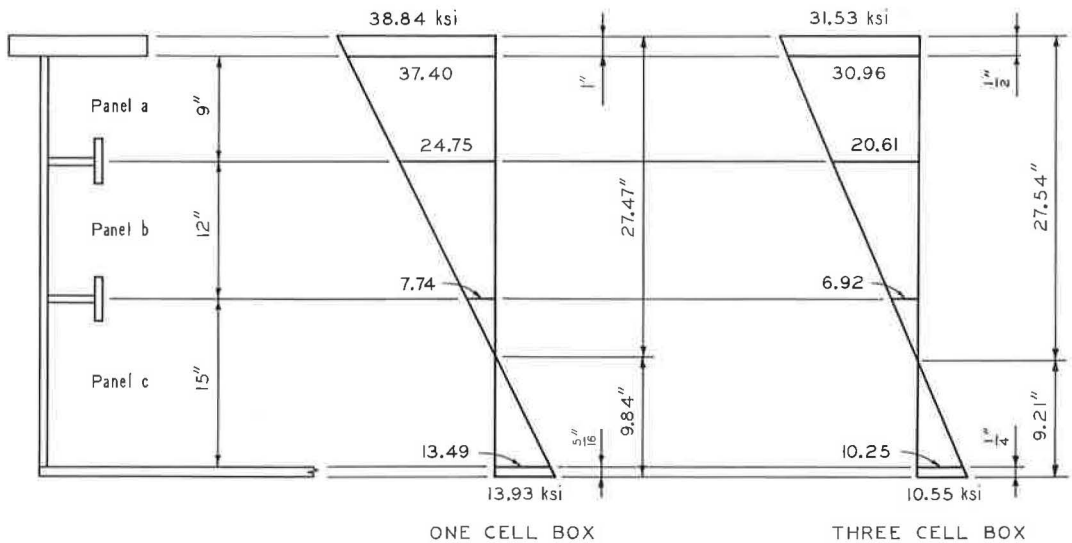


Figure 14. Setup of flexural stresses for buckling computations, 75-ft span.

TABLE 13
STABILITY OF SIDE PLATES, FLEXURAL STRESSES,
ONE-CELL BOX, 75-FOOT SPAN

Panel	k	σ_{cr} (ksi)	Ratio to Max. EFS = 38.84 ksi
a	5.3	110.9	2.75
b	6.6	77.7	2.00
c	24.0	180.8	4.65

TABLE 14
 STABILITY OF SIDE PLATES, FLEXURAL STRESSES,
 THREE-CELL BOX, 75-FOOT SPAN

Panel	k	σ_{cr} (ksi)	Ratio to Max. EFS = 31.53 ksi
a	5.2	61.2	1.94
b	6.5	43.0	2.08
c	24.0	101.7	3.22

Ratio to maximum stress in Panel b of 20.61 ksi.

TABLE 15
 STABILITY OF SIDE PLATES, SHEARING STRESSES,
 ONE-CELL BOX, 75-FOOT SPAN

Panel	τ_{cr} (ksi)	Actual τ Panel	Ratio τ_{cr} to Actual τ in Panel
a	110.9	19.72	5.6
b	62.4	19.53	3.2
c	39.9	19.10	2.1

TABLE 16
 STABILITY OF SIDE PLATES, SHEARING STRESSES,
 THREE-CELL BOX, 75-FOOT SPAN

Panel	τ_{cr} (ksi)	Actual τ Panel	Ratio τ_{cr} to Actual τ in Panel
a	62.4	13.1	4.7
b	35.1	13.0	2.7
c	22.5	12.6	1.8

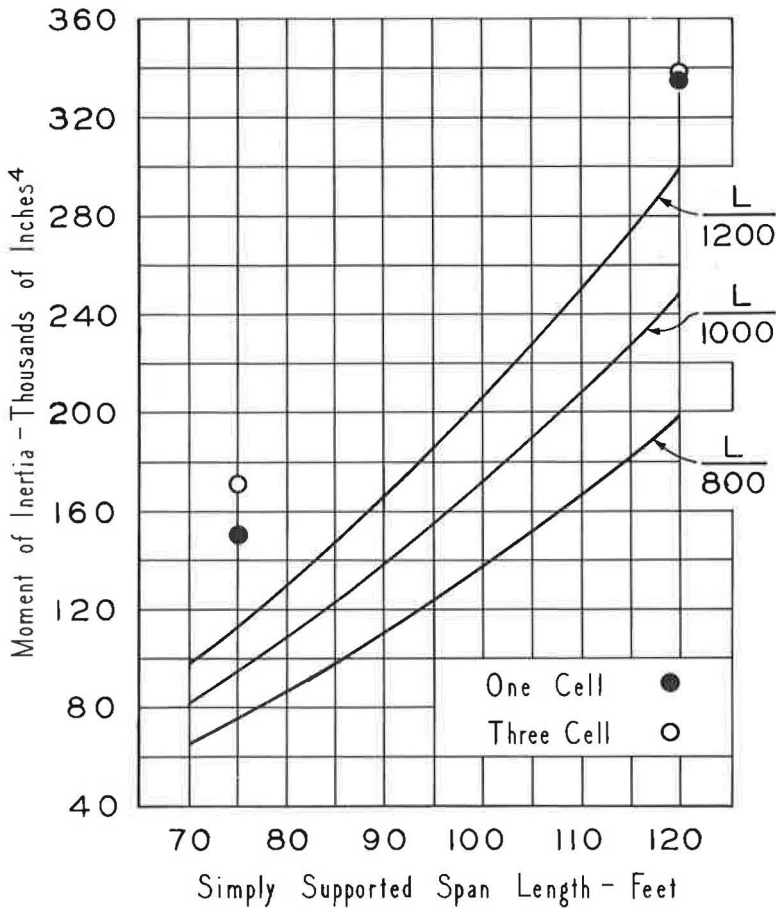


Figure 15. Deflection requirements H20-S16 live loading.

COST COMPARISONS

The structural steel quantities and cost estimates for one- and three-cell boxes on a 75-ft simple span are summarized in Tables 17 and 18. Also shown are the structural steel quantities and cost estimates for one- and three-cell boxes on a 120-ft simple span. The 120-ft span one-cell box has top flange plates of T-1 steel, 16 in. wide and $1\frac{1}{4}$ in. thick, with vertical side plates, 48 in. wide and $\frac{3}{8}$ in. thick, and a bottom plate, 16 ft wide and $\frac{1}{2}$ in. thick. The 120-ft span three-cell box has top flange plates of T-1 steel, 16 in. wide and 1 in. thick, with vertical side plates, 48 in. wide and $\frac{1}{4}$ in. thick, and a bottom plate, 24 ft wide and $\frac{5}{16}$ in. thick. The other structural details are the same as those for the 75-ft span box structures.

In Figures 16 and 17, comparisons are made with results for the rolled wide-flange and welded I-stringer structures (1, 2). The cost comparisons include the concrete roadway deck, since the quantities involved vary with the type of structure. The railings and curbs are not included in the cost estimates, as their cost would be almost identical for all the structures compared. The cost of the shear connectors for the stringers are considered to balance that of the high-strength bolts used to help hold the precast deck in position on the steel boxes. Estimates are made for the use of either ASTM A242 and A441 steels with a heat-treated constructional alloy steel, designated T-1, used for top flange plates when required by high stresses.

TABLE 17
STRUCTURAL QUANTITIES AND COST ESTIMATES
75-FOOT SPAN

Description of Structure	Type	Quantity (lb)	Structural Steel			Concrete Deck		Total Cost (\$)
			Fabrication	Erection	Freight	Quantity ¹ (cu yd)	Cost (\$)	
One Cell Box	T1, A242	46,353 ^{2,3}	9,736	2,004	695	69.42	7,636	20,871 ⁵
	T1, A441	46,353 ^{2,3}	9,134	2,004	695	69.42	7,636	20,269 ⁵
	T1, A242, SC	46,353 ^{2,3,6}	14,572 ⁷	2,004	695	69.42	7,636	25,707 ⁵
Three Cell Box	T1, A242	63,624 ^{2,3}	13,960	2,750	954	60.45	6,650	25,114 ⁵
	T1, A441	63,624 ^{2,3}	13,139	2,750	954	60.45	6,650	24,293 ⁵
	T1, A242, SC	63,624 ^{2,3,8}	19,371 ⁷	2,750	954	60.45	6,650	30,525 ⁵
Rolled WF Composite	A373	100,750				56.81	6,249	23,222
	A242	82,350				56.81	6,249	23,596
Rolled WF Non-Composite	A7	146,790				56.81	6,249	26,499
	A242	116,425			20,250	56.81	6,249	27,129
Welded-I Composite	A373	84,061				56.81	6,249	23,057
	A36	78,085				56.81	6,249	22,293
	A242	68,924				56.81	6,249	22,857
Welded-I Non Composite	A373	96,236				56.81	6,249	24,155
	A36	90,010				56.81	6,249	23,501
	A242	83,908				56.81	6,249	24,768

¹Does not include curb.

²Includes 6,181 pounds of T-1 steel.

³Does not include bearing details.

⁴Includes \$300 for bearing details.

⁵Includes \$500 for asphalt roadway surface.

⁶Includes 21,026 pounds of stainless clad steel.

⁷Includes cost of stainless clad at an extra of \$0.23 per pound.

⁸Includes 23,526 pounds of stainless clad steel.

TABLE 18
STRUCTURAL QUANTITIES AND COST ESTIMATES

Description of Structure	Type	Quantity (lb)	Structural Steel			Concrete Deck		Total Cost (\$)	
			Fabrication	Erection	Estimated Cost (\$)	Quantity ¹ (cu yd)	Cost (\$)		
									Freight
One Cell Box	T1, A242	103,823 ^{2,3}	19,825	3,875	1,557	25,557 ⁴	110.90	12,199	38,576 ⁵
	T1, A441	103,823 ^{2,3}	18,607	3,875	1,557	24,339 ⁴	110.90	12,199	37,338 ⁵
	T1, A242, SC	103,823 ^{2,3,6}	32,504 ⁷	3,875	1,557	38,236 ⁴	110.90	12,199	51,235 ⁵
Three Cell Box	T1, A242	136,328 ^{3,8}	28,055	5,090	2,045	35,490 ⁴	96.49	10,614	46,904 ⁵
	T1, A441	136,328 ^{3,8}	26,197	5,090	2,045	33,632 ⁴	96.49	10,614	45,046 ⁵
	T1, A242, SC	136,328 ^{3,8,9}	39,201 ⁷	5,090	2,045	46,636 ⁴	96.49	10,614	58,050 ⁵
Welded-I Composite	A373	207,570				36,242	90.56	9,962	46,204
	A36	189,392				34,185	90.56	9,962	44,147
	A242	170,393				36,593	90.56	9,962	46,545
Welded-I Non Composite	A373	244,476				40,241	90.56	9,962	50,203
	A36	224,052				37,596	90.56	9,962	47,558
	A242	201,358				40,352	90.56	9,962	50,314

¹ Does not include curb. ⁶ Includes 55,126 pounds of stainless clad steel.

² Includes 16,422 pounds of T-1 steel. ⁷ Includes cost of stainless clad at an extra of \$0.23 per pound.

³ Does not include bearing details. ⁸ Includes 26,275 pounds of T-1 steel.

⁴ Includes \$300 for bearing details. ⁹ Includes 48,459 pounds of stainless clad steel.

⁵ Includes \$800 for asphalt roadway surface.

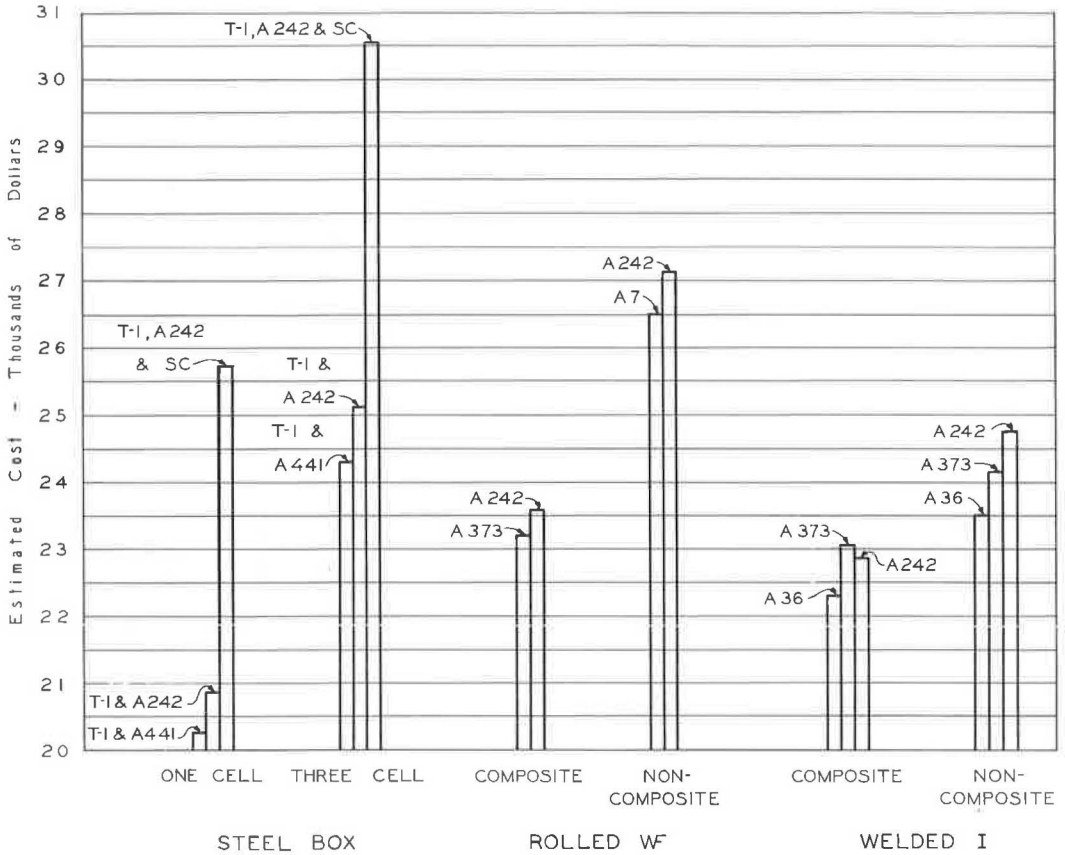


Figure 16. Cost comparison, 75-ft spans.

Cost Estimates—Steel Boxes

The fabrication cost of the steel box bridges was determined. It was assumed that the erection cost for the three-cell box would be the same as that for a welded I-stringer structure of the same length, which for the one-cell structure was computed on a tonnage ratio with the three-cell structure. Freight was taken as \$0.015/lb. The cost of steel bearing details was assumed to be \$300.00 for each of the steel box structures.

An estimate was made using stainless-clad steel for the outside side and bottom plates, as well as the outside longitudinal splice plate and the seal plates at the ends of the bridge. The base price for the stainless-clad material, after consultation with two leading manufacturers of stainless-clad plate, was taken as \$0.2665/lb. This compares with \$0.0785 as the base price of nickel-copper ASTM A242 steel. The fabricating costs for the stainless-clad plates were assumed to be about one-third higher than for plates of A242 steel. This gave an additional cost of \$0.23/lb for the stainless-clad plates over those of A242 steel. Structural T's were used for the longitudinal stiffeners and the stiffening rings in the cost estimates.

The asphalt wearing surface on the precast decks for the steel box structures was estimated at \$2.00/sq yd of roadway area.

Comparisons

The estimated cost of the one-cell box structure with the 75-ft simple span is less than the lowest cost structure with either rolled wide-flange or welded I-stringers,

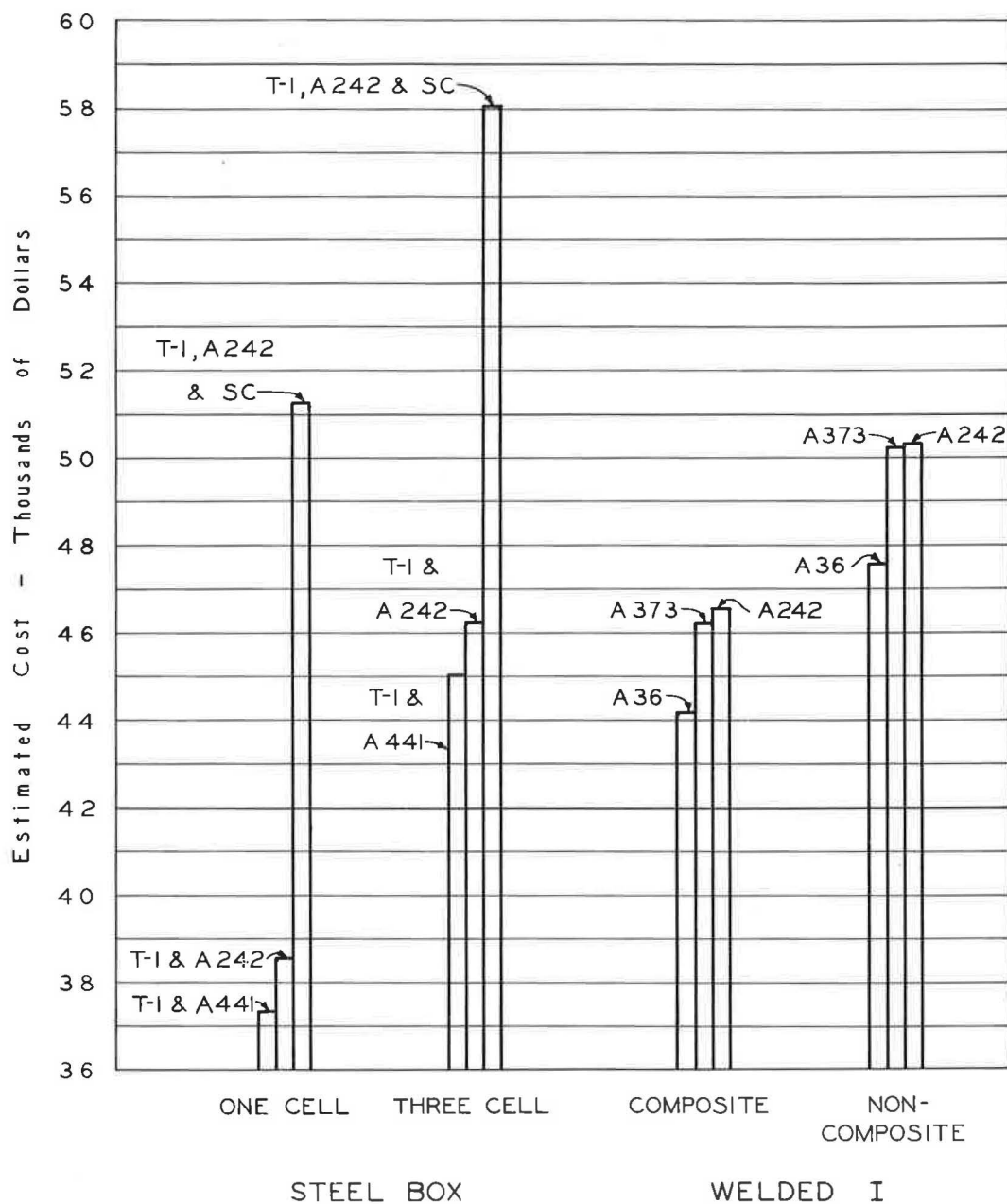


Figure 17. Cost comparisons, 120-ft spans.

except when stainless-clad steel is used in the outside plates. However, the three-cell box structure has, in general, a slightly higher estimated cost.

The estimated cost of the one-cell box structure with the 120-ft simple span is also less than the lowest cost for the welded I-structure, except when stainless-clad steel is used for the outside plates. The three-cell box structure has, in general, a slightly higher estimated cost, but the difference is less than in the case of the 75-ft simple span.

These estimates do not reflect any possible long-term maintenance savings due to the increased resistance to atmospheric corrosion or the better paint life of nickel-copper types of high-strength low-alloy steels.

CONCLUSIONS

The results of this study indicate that the steel box structure with a precast concrete deck has definite economic possibilities for use as a highway bridge. It is recommended that a nickel-copper type of high-strength low-alloy steel be used for these structures because of its better resistance to atmospheric corrosion (1), since thin plates are proposed. It should be noted that a heat-treated constructional alloy steel, designated T-1, is used for top flange plates where required.

ACKNOWLEDGMENTS

This study was made in the Engineering Experiment Station, Purdue University, in cooperation with the International Nickel Co. The authors gratefully acknowledge the assistance of F. W. Schroeder and J. F. W. Koch of the International Steel Co., Evansville, Ind., for their assistance in making the cost estimates and wish to thank L. Anselmini of the International Nickel Co. for his assistance in the investigation and the preparation of this report. David R. Raab, graduate assistant, helped in the final phases of this project.

REFERENCES

1. Hayes, J. M., and Maggard, S. P. Economic Possibilities of Corrosion-Resistant Low Alloy Steel in Short Span Bridges. Proc. A.I.S.C. Nat. Eng. Conf., pp. 59-68, 1960.
2. Hayes, J. M., and Maggard, S. P. Economic Possibilities of Corrosion-Resistant Low-Alloy Steel in Welded I-Section Stringer Highway Bridges. Highway Research Board Proc., Vol. 41, pp. 125-162, 1962.
3. Dörnen, K., and Meyer, A. Die Emsbrücke in dübellosem Stahlverbund. Der Stahlbau, pp. 199-206, July 1960.
4. Sattler, K. Betrachtungen über die Verwendung hochzugfester Schrauben bei Stahlträger-Verbundkonstruktionen. Preliminary Publ., 6th Congr. Int. Assoc. for Bridge and Structural Eng., pp. 333-350, 1960.
5. Postl, J. Klebung bei einer Verbundbrücke. Der Bauingenieur, pp. 390-391, Oct. 1962.
6. Epoxy Bonding Compounds as Shear Connectors in Composite Beams. New York Dept. of Public Works, Interim Rept., Physical Res. Proj. No. 13, Eng. Res. Ser. RR 62-2, Oct. 1962.
7. Seely, F. B., and Smith, J. O. Advanced Mechanics of Materials. 2nd Ed., New York, John Wiley and Sons, 1952.
8. Murphy, Glenn. Advanced Mechanics of Materials. 1st. Ed., New York, McGraw-Hill, 1946.
9. Bryan, G. H. On the Stability of a Plate under Thrusts in Its Own Plane with Application on the Buckling of the Sides of a Ship. Proc. London Math. Soc., Vol. 22, pp. 54-57, 1891.
10. Timoshenko, S. P., and Gere, J. M. Theory of Elastic Stability. 2nd Ed., New York, McGraw-Hill, 1961.
11. Bleich, F. Buckling Strength of Metal Structures. New York, McGraw-Hill, 1952.
12. Maggard, S. P. The Structural Analysis of Box-Like Girders for Highway Bridges. Unpubl. doctoral diss., Purdue Univ., Jan. 1963.
13. Kollbrunner, C. F., and Meister, M. Ausbeulen, Theorie und Berechnung von Blechen. Berlin, Springer-Verlag, 1958.
14. Rockey, K. C. Web Buckling and the Design of Web Plates. Brit. Aluminum Devel. Assoc., Res. Rept. No. 36, Sept. 1958.

15. Massonnet, C. Experimental Research on the Buckling Strength of the Webs of Solid Girders. Preliminary Publ., 4th Congr. Int. Assoc. for Bridge and Structural Eng., pp. 539-555, 1952.
16. AASHO. Standard Specifications for Highway Bridges. 8th Ed., 1961.